NEURAL COMPUTATION OF SELF-MOTION FROM OPTIC FLOW IN PRIMATE VISUAL CORTEX

Thesis by

Brian Lee

In Partial Fulfillment of the Requirements for the

Degree of

Doctor of Philosophy

California Institute of Technology

Pasadena, California

2006

(Defended May 17, 2006)

DEDICATION

For my dear family: my mother, my father, and my brother.

ACKNOWLEDGEMENTS

"God saw all that he had made, and it was very good."
Genesis 1:31

First and foremost, I would like to thank my advisor, Richard Andersen, who took a chance and gave me the wonderful opportunity to work in his laboratory. His knowledge, support, and guidance has been instrumental in my growth as a young scientist. To my committee members, Shinsuke Shimojo, Christof Koch, and Joel Burdick, your critical insights have been valuable in guiding my experiments and analysis. I also had the privilege to work with Bijan Pesaran, my main collaborator, who has been extremely generous with his time, data analysis expertise, and surgical experience. Thank you for allowing me to bother you with endless questions!

I would also like to thank all the members of the Andersen laboratory who have made life in the lab so interesting, enjoyable, and colorful. Who will ever forget our weekly "Color Days"? Thanks to Kelsie Pejsa, Nicole Sammons, and Lea Martel for animal care and surgery room conversations, Tessa Yao for USC/UCLA banter (Go Trojans!), Viktor Shcherbatyuk for fun with computers, James A. Crowell for optic flow stimulus assistance, and Marina Brozovic and Boris Breznen for scientific discussions. Thanks to Zoltan Nadasdy for being a good rig-mate and Grant Mulliken for the many unforgettable adventures.

Thanks to my friends for their support and friendship over the past five years. Finally, I would like to give a huge "Thank You!" to my family: my mother, my father, and my brother, for their love, endless support, and encouragement. I couldn't have done any of this without you.

This work was supported by the National Eye Institute, J.G. Boswell Professorship, a Career Award in the Biomedical Sciences from the Burroughs Wellcome Fund, and a Howard Hughes Medical Institute Pre-Doctoral Fellowship.

ABSTRACT

Area MSTd is involved in the computation of heading direction from the focus of expansion (FOE) of the visual image. Our laboratory previously found that MSTd neurons adjust their focus tuning curves to compensate for shifts in the FOE produced by eye rotation (Bradley et al., 1996) as well as for changes in pursuit speed (Shenoy et al., 2002). The translation speed of an observer also affects the shift of the FOE. To investigate whether MSTd neurons can adjust their focus tuning curves to compensate for varying translation speeds, we recorded extracellular responses from 93 focus-tuned MSTd neurons in two rhesus monkeys (*Macaca mulatta*) performing pursuit eye movements across displays of varying translation speeds. We found that MSTd neurons had larger shifts in their tuning curves for slow translation speeds and smaller shifts for fast translation speeds. These shifts aligned the focus tuning curves with the true heading direction and not with the retinal position of the FOE. These results indicate that retinal cues related both to translation speed and extraretinal signals from pursuit eye movements are used by MSTd neurons to compute heading direction.

Although there is much evidence that MSTd neurons are involved in heading computation, it was not known in which coordinate frame the tuning curves were represented. We performed a second set of experiments to determine whether focus tuning curves in area MSTd were represented in eye, head, body, or world coordinates. The coordinate frame was determined while the eyes were stationary (fixed gaze, simulated pursuit condition) and while the eyes were moving (real pursuit condition). We recorded extracellular responses from 80 MSTd neurons and found that the FOE tuning curves of the overwhelming majority of neurons were aligned in an eye-centered coordinate frame as opposed to head, body, or world-centered coordinates (fixed gaze: 77/80 (96%); real pursuit: 77/80 (96%); simulated pursuit 74/80 (93%); t-test, $p<0.05$). We also found that area MSTd demonstrated significant eye position gain modulation much like its posterior parietal neighbors. This gain modulation may be a method of transforming eye coordinates into other coordinate frames at later stations of the nervous system.

TABLE OF CONTENTS

LIST OF FIGURES AND TABLES

FIGURES:

TABLES:

Chapter 1: Introduction

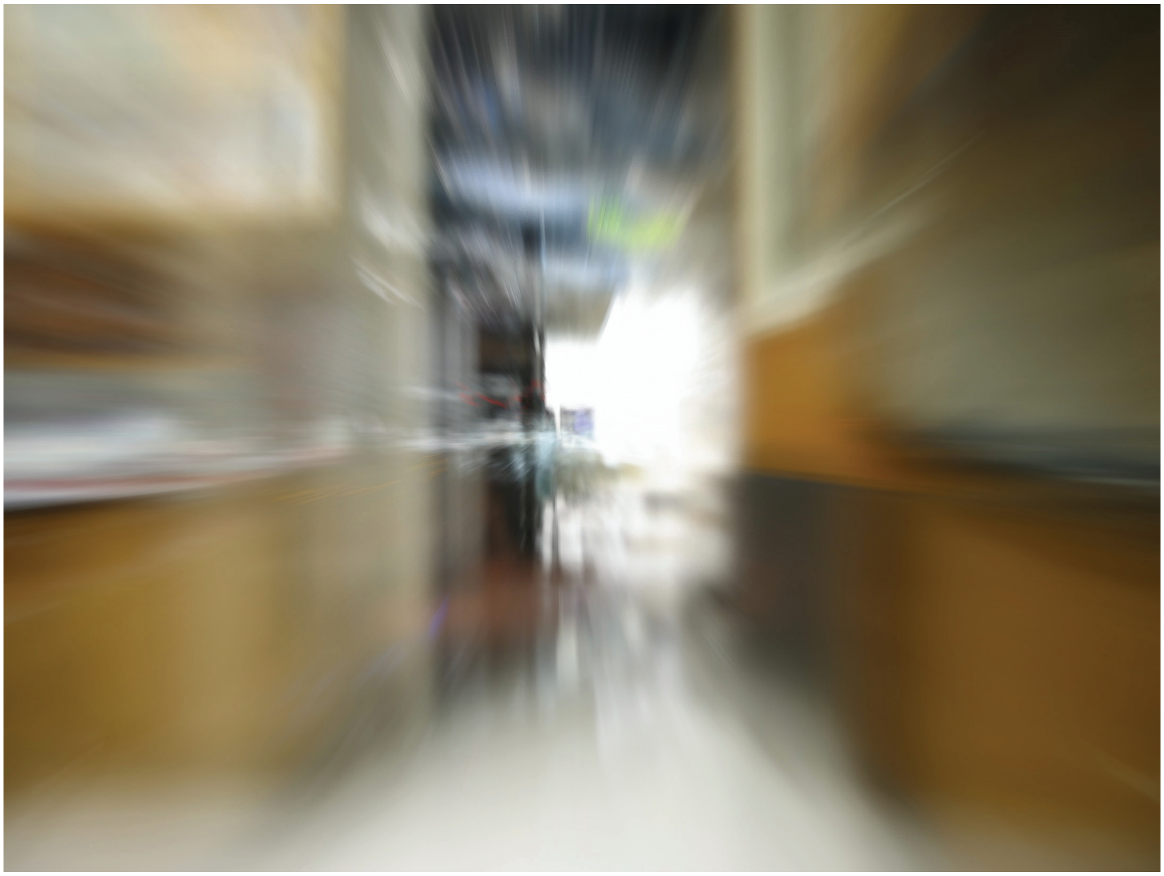

Figure 1-1 Optic Flow Generated by Forward Motion
Walking down the hallway generates optic flow on the retina. Peripheral objects appear to radiate out from a central point called the focus of expansion (FOE). We can use the FOE to determine the direction of heading. These complex signals are processed in specialized areas of the brain such as the dorsal aspect of the medial superior temporal area (MSTd).

1.1 Theories of Heading Computation

How do we know which way we are moving as we walk through the environment? Clearly, we depend heavily upon vision to plan and guide our intended movements. Gibson suggested that for an individual in motion, the focus of expansion (FOE) of the retinal image could be used to determine the direction of heading (Gibson, 1950). The

FOE is the point from which the visual image appears to expand. Figure 1-1 When the eyes are stationary, the FOE corresponds to the instantaneous direction of movement, which is the heading direction. However, when eye and head movements are present, the focus of expansion no longer corresponds with the heading direction (Longuet-Higgins and Prazdny, 1980; Koenderink and van Doorn, 1986). To appreciate this, imagine an observer walking down the road while their eyes are fixating on an airplane flying across the horizon from left to right. As the observer moves forward and follows the moving plane with their eyes, the eyes rotate in the head. This eye movement adds a laminar motion to the forward translation component of the visual field that is in the opposite direction of the eye movement. As a result, the retinal focus of expansion is shifted in the direction of eye movement and no longer indicates the true heading direction. Figure 1-2

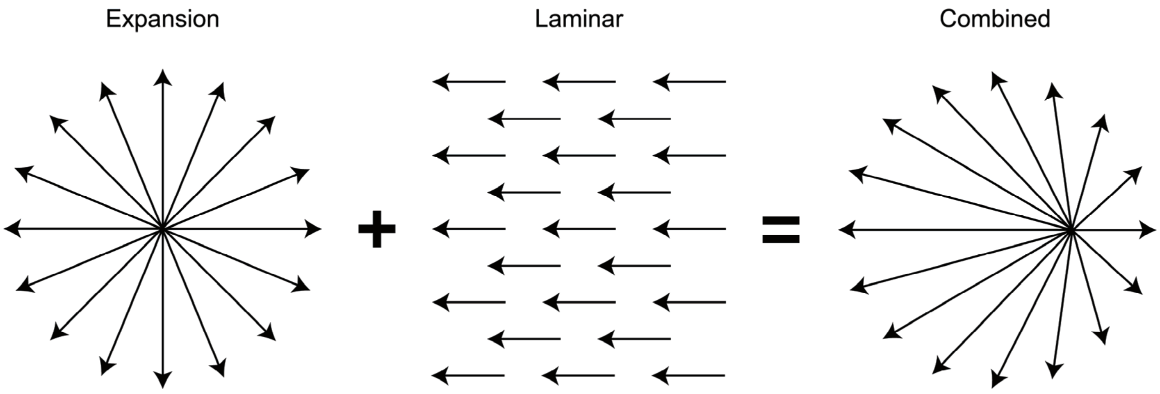

Figure 1-2 Retinal Image During Forward Motion and Eye Rotation
When we move forward, the visual world appears to expand. If the eyes are not moving, the focus of expansion indicates the direction of heading. However, smooth pursuit to the right adds a leftward laminar motion and shifts the focus of expansion in the direction of pursuit.

Theoretically, the true focus of expansion, which represents the actual heading direction, could be found by separating the visual flow field into its basic components of forward translation and rotation due to pursuit eye movement. Once separated, the forward translation component would indicate the true direction of heading (Longuet-Higgins and Prazdny, 1980). For scenes with depth cues, the same decomposition methods could apply, although the flow patterns during eye movements are more complicated.

1.1.1 Optic Flow Decomposition Methods

Two methods have been proposed on how the visual motion generated upon the retina, which is known as optic flow, could be decomposed into separate translational and rotational components. One method utilizes the retinal cues in the visual scene, such as motion parallax, and the other uses extraretinal cues, such as an efference command signal related to pursuit eye movements, to adjust templates matched to optic flow patterns.

1.1.1.1 Retinal Cues

Early computational models attempted to use solely retinal cues to recover the heading direction from optic flow (Longuet-Higgins and Prazdny, 1980; Koenderink and van Doorn, 1981; Rieger and Lawton, 1985; Hildreth, 1992). These models segmented the visual scene and analyzed local regions for their flow patterns. These models suggested that the areas of the brain that analyze optic flow could use simple types of motion patterns as a basis set for more complex motion. These models were able to take visual scenes that were perturbed by eye movements and recover the pure expansion component. However, the techniques were based upon general algorithms using retinal cues to analyze optic flow, and were not specific about how they could be implemented in the brain in a biologically plausible manner.

1.1.1.2 Template Models

The second class of models was developed to perform optic flow decomposition in a more biologically realistic manner (Hatsopoulos and Warren, 1991; Lappe and Rauschecker, 1994; Perrone and Stone, 1994; Warren, 1995; Stone and Perrone, 1996). These models use receptive fields to match various flow patterns and are known as template models. According to these models, brain areas that process vision contain templates for the various optic flow conditions that result from different eye rotation speeds, translation speeds, depth variations, and structure in the scene. In order to represent all possible optic flow patterns, templates representing one variable of the optic flow need to be multiplied by the number of templates representing another aspect of the optic flow. As a result, these models require a large number of templates, and thus a criticism of the models is that they necessitate the use of too many neurons to be biologically plausible.

An interesting method of reducing the number of templates needed to represent self-motion would be to use an extraretinal signal to adjust the templates dynamically. This extraretinal signal, or efference copy, could be a copy of the motor commands to move the eyes. This would considerably reduce the number of templates required. Human psychophysical experiments have demonstrated that eye rotations can be compensated for by an extraretinal signal representing pursuit speed and pursuit direction (Royden et al., 1992; Royden et al., 1994). This supports the idea that a smaller number of templates can be dynamically adjusted via an external eye position signal to represent the perturbation of the visual field due to eye movement instead of having a large number of templates representing every possible optic flow scenario (Andersen et al., 1996).

1.2 Psychophysics

1.2.1 Fixed Gaze

In order to study Gibson's original proposal that optic flow could be used for navigation, many psychophysical studies have been performed to examine whether human subjects could determine heading direction from optic flow. Experiments by Warren et al. required subjects to view random dot ground plane stimuli simulating forward translation. They found that the subjects were able to make accurate heading judgments if there were no eye or head rotations (Warren and Hannon, 1988). However, these conditions are not realistic, as we often move our eyes as we navigate through the environment.

1.2.2 Eye Pursuit

Using more realistic conditions, Banks and colleagues examined heading accuracy when subjects performed smooth pursuit eye movements across ground plane stimuli. They found that subjects were still able to make accurate heading judgments even though eye pursuit adds laminar motion to the visual stimulus and shifts the focus of expansion away from the true heading direction (Royden et al., 1992; Royden et al., 1994).

1.2.3 Simulated Pursuit

However, they found that if they simulated eye movements by adding laminar motion directly to the stimulus, the subjects were no longer able to accurately judge their heading direction (Royden et al., 1992; Royden et al., 1994). Since the retinal image was the same in the real and simulated pursuit conditions, this result indicated that the actual eye movement is necessary for accurately estimating heading direction. Somehow, the extraretinal pursuit signal allows the subject to compensate for the shift of the visual image and determine the correct heading direction and appears to be necessary to decompose the retinal image into its translation and eye rotation components. The fact that humans are not very good at making heading estimates from stimuli that simulate pursuit eye movements was recently confirmed again by Crowell and Andersen, (2001).

1.2.4 3-Dimensional Visual Stimuli

The aforementioned studies primarily used ground plane stimuli that contain 3D retinal cues such as motion parallax. However, other human psychophysical studies have used 2D frontoparallel stimuli that simulate approach to a wall (Warren and Hannon, 1990; Royden et al., 1994). These studies also found complete compensation for pursuit eye movements across a 2D frontoparallel stimuli, results which are similar to those using a 3D ground plane stimuli. However, Crowell et al. recently duplicated those experiments, and did not find complete pursuit compensation for frontoparallel stimuli (Crowell and Andersen, 2001). They carefully monitored eye movements and found that the subjects often slowed their pursuit eye movements near the end of a trial, just before estimating their heading direction. When those trials were discarded, they found the subjects only partially compensated for the shifted FOE. Previous studies did not monitor eye movement, and it is possible that there was less retinal focus shift than had been assumed. Interestingly, when the frontoparallel stimuli were replaced with simulated translation over a ground plane, Crowell et al. found complete compensation as had been reported previously. From this study, it appears that 3D retinal cues, such as motion parallax, improve compensation.

1.2.5 Movement Towards a Target Location

Some investigators agree with the findings that optic flow can be used for navigation but question whether it is the primary source of information during locomotion in the natural environment (Rushton et al., 1998; Harris and Rogers, 1999). They point out that humans are able to navigate in situations where optic flow information is minimal, such as walking at night, or during snowstorms, where the flow information is incorrect. They suggest that subjects simply move towards a goal or landmark. Warren and colleagues recently explored this possibility by having subjects walk through a virtual environment where the optic flow could be manipulated independently from the direction of locomotion. They found that the subjects did use the location of the goal or target for locomotion, but increasingly used optic flow as its magnitude was increased in the display. They concluded that navigation used both movement towards a goal and optic flow, depending on the environmental conditions (Warren et al., 2001).

1.2.6 Head Rotation

To examine whether humans can use optic flow for navigation, the previous psychophysical studies examined the effects of pursuit eye movement on the ability of human subjects to determine heading direction. In addition to pursuit eye movements, the visual image can also be perturbed by pursuit head movements. Commonly, pursuit movements are often made with both the head as well as the eyes, especially for large gaze shifts. If humans do in fact use optic flow for navigation, then they should be able to compensate for changes in the visual image caused by head movement, just as they can for eye movements. Crowell et al. performed experiments where subjects pursued by turning their heads across displays that simulated translation over a ground plane. The subjects were able to judge their direction of heading equally well during head movements as they did with eye movements (Crowell et al., 1998).

Furthermore, they performed experiments to determine the source of the extraretinal signal used to compensate for head movements. The extraretinal signal could have come from vestibular signals, neck proprioceptive signals, or the efference copy of the head turn. They found that there was no compensation when only vestibular or only neck proprioceptive signals were present. However, the presence of two signals produced partial compensation. When all three cues were available complete pursuit compensation was achieved (Crowell et al., 1998).

1.3 Dorsal Aspect of the Medial Superior Temporal Area

1.3.1 Dorsal and Ventral Stream

Lesion studies have contributed significantly to the understanding of how visual information is processed in the brain. Studies have shown that lesions in the inferotemporal cortex lead to a loss of recognition functions and deficits in object discrimination tasks (Aggleton and Mishkin, 1990) while damage to the posterior parietal cortex results in neglect, visual mislocalization, visual disorientation, oculomotor deficits, and loss of spatial memory (Andersen, 1987; Karnath et al., 1991; Braun et al., 1992). Based upon these studies in humans and nonhuman primates, Ungerleider and Mishkin proposed that visual processing was split into two distinct streams that ran parallel to each other: a dorsal "what" stream and a ventral "where" stream (Ungerleider and Mishkin, 1982). Figure 1-3 Both streams originate from the primary visual cortex with the dorsal stream leading to the posterior parietal cortex and the ventral stream to the inferotemporal cortex. They suggested that the ventral "what" stream was involved in the processing of object information while the dorsal "where" steam was involved in spatial information processing (Goodale and Milner, 1992).

A critical part of the dorsal stream that is involved in self-motion processing is the medial superior temporal area (MST), which lies in the superior temporal sulcus. Area MST is divided into two distinct regions: MSTd (dorsal) and MSTl (lateral) (Desimone and Ungerleider, 1986; Saito et al., 1986; Ungerleider and Desimone, 1986a, b; Komatsu and Wurtz, 1988a). Neurons in MSTl have smaller receptive fields than those in MSTd and are thought to play a role in target selection during smooth pursuit eye movements (Komatsu and Wurtz, 1988a) while MSTd neurons are responsive to various elements of optic flow. We will now focus on area MSTd and review a broad array of research that indicates that MSTd plays a role in computing heading direction from visual motion.

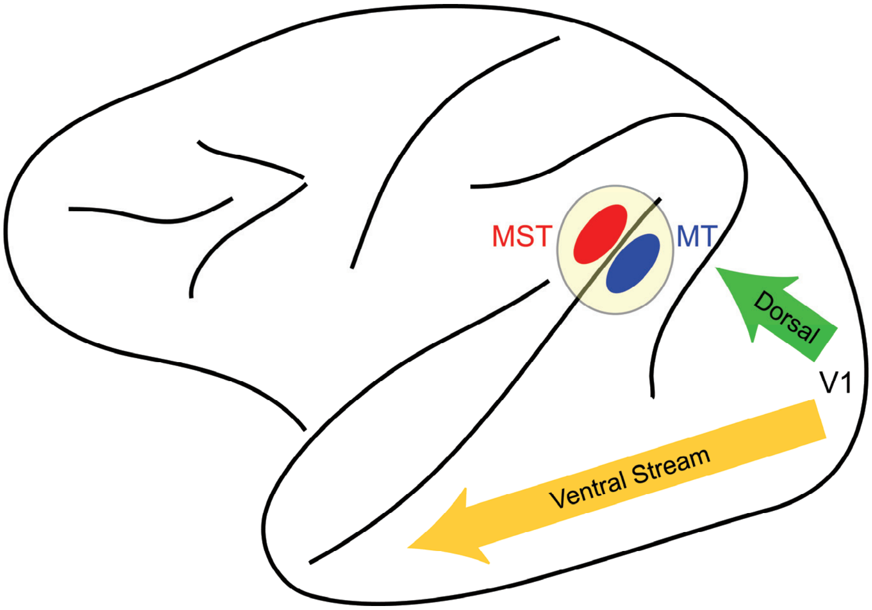

Figure 1-3 Location of Area MST and the Dorsal and Ventral Streams
Area MST and MT are located in the superior temporal sulcus. Both the dorsal and ventral streams begin at V1. The dorsal "where" stream leads to the posterior parietal cortex, while the ventral "what" stream proceeds to the inferotemporal cortex.

1.3.2 Discovery of Area MSTd

Researchers discovered that neurons in MSTd were responsive to complex motion patterns such as expansion, contraction, and rotation (Sakata et al., 1985; Saito et al., 1986; Sakata et al., 1986; Tanaka et al., 1986; Tanaka et al., 1989; Tanaka and Saito, 1989; Sakata et al., 1994). These motion patterns are similar to those generated by self-motion and led many investigators to propose that area MSTd is involved in navigation from optic flow. There was additional support for the idea when it was found that the receptive fields of expansion selective neurons in MSTd were tuned to the location of the focus of expansion of the visual image (Duffy and Wurtz, 1995).

1.3.3 Spiral Space

While some MSTd neurons were sensitive to just one motion pattern, Duffy and Wurtz found that several neurons were responsive to more than one motion pattern. Some MSTd neurons responded to expansion, expanding spirals, and rotations (Duffy and Wurtz, 1991b, a). This observation led to the idea that area MSTd was not using discrete or a basis set of motion patterns but instead a continuum of motion patterns to represent optic flow.

Graziano et al., (1994) performed experiments to determine whether neurons in MSTd represented optic flow in discrete patterns or along a continuum. They examined the response of MSTd neurons to a category of visual motion patterns known as spiral space. Spiral space is constructed by rotating the motion vectors in an expansion stimulus by different counterclockwise angles (0° for expansion, 45° for a counterclockwise-expanding spiral, 90° for counterclockwise rotation, 135° for a counterclockwise-contracting spiral, 180° for contraction, 225° for a clockwise-contracting spiral, 270° for clockwise rotation, and 315° for a clockwise-expanding spiral). Figure 1-4 Expansion and contraction are represented on the vertical axis, and clockwise/counterclockwise rotation on the horizontal axis. If area MSTd is sensitive to discrete patterns, then one would expect that neurons in MSTd would only respond to cardinal motions of expansions, contractions, and rotations. However, if MSTd neurons represent optic flow along a continuum, then the neurons, in addition to being sensitive to cardinal motion, would also respond to combinations of motions such as expanding spirals (expansion + rotation), or contracting spirals (contraction + rotation). Graziano et al. found that many MSTd neurons were responsive to the whole continuum of spiral space. When plotted as a tuning curve, they found that MSTd neurons typically had a smooth, single-peaked tuning curve. This was evidence that neurons in MSTd did in fact represent spiral space along a continuum and not a discrete set of patterns.

Orban and colleagues came to a similar conclusion after examining MSTd neurons that were sensitive to expansion. The found that adding rotational motion into an expanding flow field, and thereby creating a spiral, decreased the response magnitude of certain MSTd neurons (Orban et al., 1992). The neurons were not as responsive to spiral motion as they were to pure expansion patterns. If neurons in MSTd were extracting the expansion component from complex optic flow, then it should not have mattered if rotational motion were added. This result supported the findings of Graziano et al. that

MSTd neurons encoded motion along a continuum and were not extracting expansion motion from optic flow.

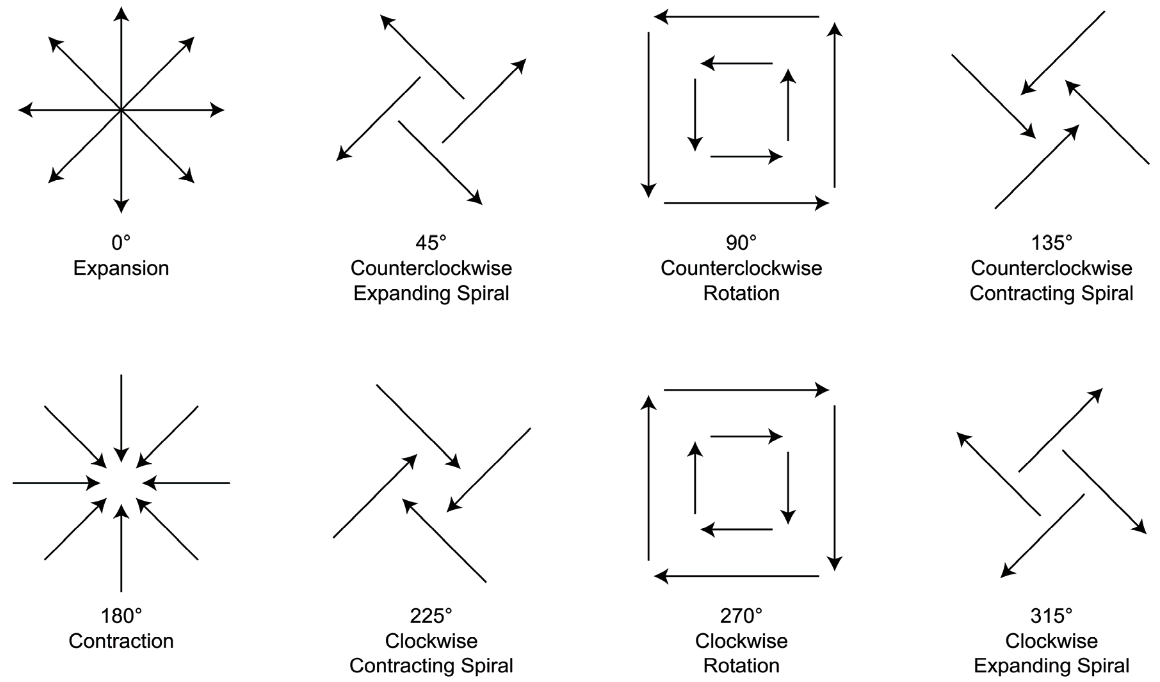

Figure 1-4 Spiral Space
Spiral space is constructed by rotating the motion vectors in an expansion stimulus by different counterclockwise angles: 0° for expansion, 45° for a counterclockwise-expanding spiral, 90° for counterclockwise rotation, 135° for a counterclockwise-contracting spiral, 180° for contraction, 225° for a clockwise-contracting spiral, 270° for clockwise rotation, and 315° for a clockwise-expanding spiral.

1.3.4 Smooth Pursuit Sensitivity

Studies have found that MSTd neurons are responsive when monkeys make smooth pursuit eye movements. In addition, they found that as the speed of eye pursuit increased, the neural discharge rates from MSTd neurons increased as well (Komatsu and Wurtz, 1988a). Not only were MSTd neurons responsive to the speed of pursuit, but also to the direction of pursuit. Several studies have found activity related to the direction of smooth pursuit in area MSTd (Lynch et al., 1977; Komatsu and Wurtz, 1988b, a;

Newsome et al., 1988; Warren, 1995). As the pursuit direction was varied, the MSTd neurons modulated their firing rates and demonstrated preferred/null directions of pursuit. Having both optic flow and eye pursuit response in area MSTd hinted that this area was involved in heading computation.

1.3.5 Form/Cue Invariance

If area MSTd was involved in self-motion perception, then one would expect that the neurons would be sensitive to optic flow motion regardless of the form or cue types in the visual scene. For example, running through the forest compared to running through a dense city would create the same retinal flow pattern, yet the visual forms and cues are very different. As a region of the brain that might be involved in heading perception, the neurons would be expected to demonstrate form and cue invariance. From a template model point of view, it would be more economical to have single templates coding individual motion patterns, instead of a variety of templates, each coding the same motion patterns, but for cues of different forms. Geesaman et al. found that MSTd neurons exhibited the same pattern selectivity regardless of whether the motion pattern was provided by a single object, random dot patterns, or even non-Fourier motion (Geesaman and Andersen, 1996). Although the magnitude of the response would vary depending upon the stimuli used, the preferred motion pattern generally remained the same.

1.3.6 Map for Optic Flow Selectivity in Area MSTd

Several investigators have noted that MSTd neurons appear to be arranged in clusters that share the same preferred motion pattern. Gessamen et al., (1997) examined this issue using a double-label 2-deoxyglucose technique. The monkeys were shown one motion pattern in the presence of ^{3}H-labeled 2-deoxyglucose and then a second motion pattern was shown during the injection of ^{14}C-labeled 2-deoxyglucose. In their study they tested two pairs of optic flow stimuli, expansion and contraction, or expansion and rotation. For both pair of optic flow stimuli, they found interdigitated columns within MSTd for the two labels. However, the interdigitation was more prominent and widely spaced for expansion/contraction than for expansion/rotation. This suggested that optic flow selectivity was organized in a columnar fashion in MSTd. The results are in agreement with the finding that neurons in MSTd represent spiral space in a continuous fashion (Graziano et al., 1994). They are also in agreement with the observation that the flow patterns of expansion and contraction are maximally separated on a 360° mapping of spiral angles. It appears that the spiral mapping is also present anatomically in area MSTd. In a separate study using electrophysiological techniques, Britten found that neurons that are close to each other have more similar optic flow tuning preferences than neurons that are far apart (Britten, 1998).

1.3.7 3D Cues

Upadhyay et al. found that adding 3D cues such as motion parallax to optic flow displays produced larger responses in MSTd neurons when compared to 2D frontoparallel stimuli. With 3D cues, they found that MSTd neurons not only increased their response, but also displayed stronger heading selectivity (Upadhyay et al., 2000). This finding was similar to psychophysical studies which found that humans are able to make more accurate heading judgment during pursuit across stimuli that contain 3D cues than across those with 2D cues (Crowell and Andersen, 2001).

1.3.8 Microstimulation

If area MSTd is involved in heading perception, then perturbing the local activity by microstimulation should bias the perceived direction of movement. Britten et al. found that microstimulation of MSTd neurons while monkeys made heading judgments biased their perceived heading. They also performed microstimulation when the monkeys were making pursuit eye movements across the stimulus. During pursuit, the heading bias was the most robust. This suggested that area MSTd was where optic flow and pursuit signals converged for heading direction calculations (Britten and van Wezel, 1998).

1.4 Heading Experiments in Area MSTd

1.4.1 Pursuit Compensation

Inspired by psychophysical experiments that showed that the extra retinal signal of eye pursuit could compensate for eye rotations (Royden et al., 1992; Royden et al., 1994), Bradley et al., (1996) designed experiments that examined the role of extraretinal signals from pursuit eye movements in compensating for motion on the retina during self-motion. Studies had shown that neurons in MSTd were responsive to the direction and speed of eye pursuit movements (Kawano et al., 1984; Newsome et al., 1988; Kawano et al., 1994). It was possible that this pursuit sensitivity could be used to shift the focus tuning curves of MSTd neurons during pursuit eye movements.

In the experiments by Bradley et al., (1996), they first generated focus tuning curves of MSTd neural activity with the eyes stationary. In this fixed gaze condition the focus tuning curve represents the actual heading direction. In the pursuit condition, the monkey pursued a moving target along the preferred or anti-preferred direction of the neuron, which was determined earlier. The visual stimulus was exactly the same between the fixed condition and the pursuit condition. Data for the tuning curves was recorded while the eyes were passing through the straight ahead position on the screen. In this manner, the eye positions in both the fixed and pursuit condition were approximately the same. However, the eye rotation generated a laminar motion that combined with the expansion stimuli and shifted the focus of expansion on the retina in the direction of the pursuit eye movement. Figure 1-2 Therefore, the retinal image between the fixed gaze condition and the real pursuit condition was shifted because of the pursuit eye movement.

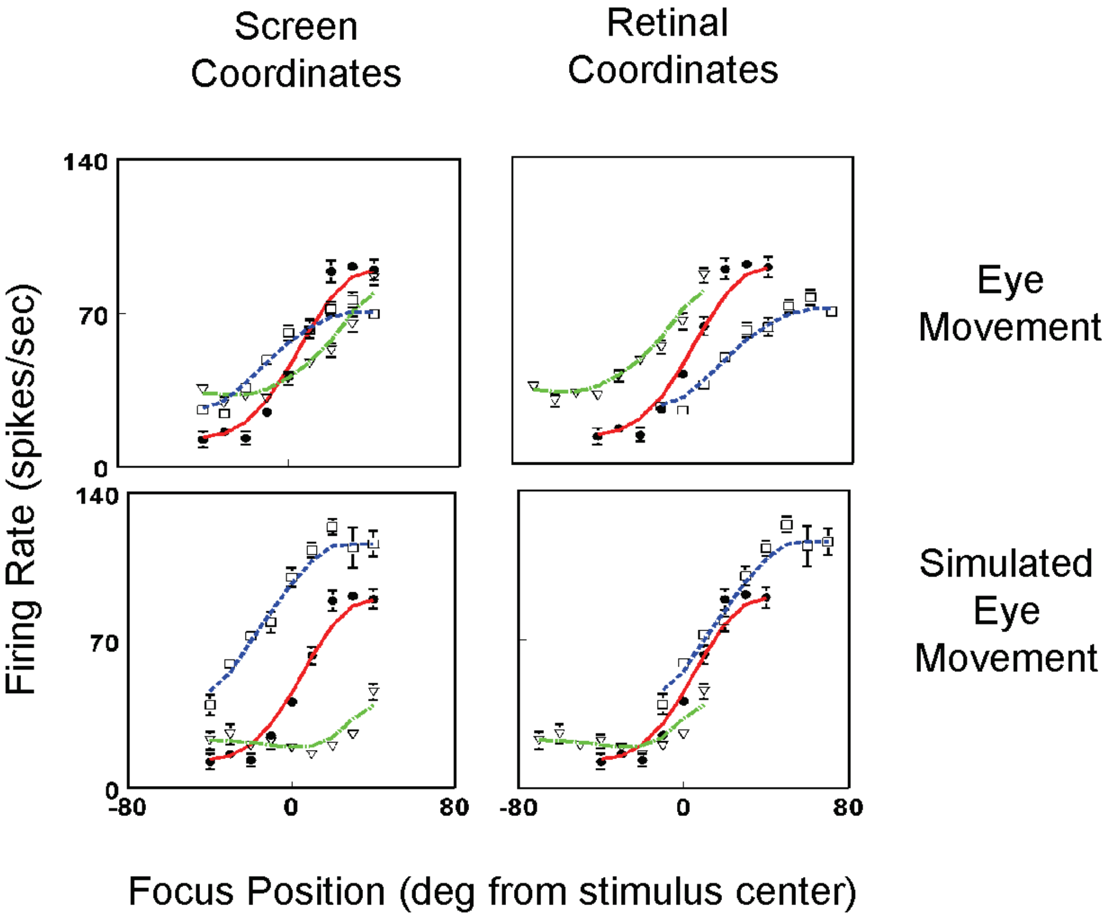

Figure 1-5 MSTd Heading Neuron
Red lines and solid circles represent fixed gaze focus tuning curves. Blue lines and open squares are preferred direction eye movements (real or simulated). Green lines and open triangles are anti-preferred direction eye movements (real or simulated). Data in the left and right columns are identical, except that the pursuit curves in the right column were shifted by 30° relative to screen coordinates (thus giving retinal coordinates). The moving-eye focus tuning curves align in screen coordinates (top left panel) and thus encode the direction of heading. However, for simulated eye movements, the fields align in retinal coordinates. From Bradley et al., (1996).

Interestingly, when they examined the focus tuning curves from the fixed and real pursuit condition, they found that when plotted in retinal coordinates, the tuning curves did not align; however, when plotted in screen coordinates, the tuning curves overlapped each other closely. Figure 1-5 This meant that the neurons represented the same focus location on the screen regardless of whether the eyes were stationary or moving. This was unique since the retinal images were different, yet the tuning curves were similar. One would expect the tuning curves to be shifted by the same amount as the pursuit shifted retinal image. This indicated that in the real pursuit condition, the MSTd neurons were able to take the retinal image that was shifted due to pursuit eye movements and shift the tuning curves in the proper direction to align with the fixed gaze tuning curve which represents heading direction.

In another condition, the monkey fixated straight ahead and the stimulus window was drifted across the screen in the direction opposite of pursuit. Again, data was collected while the stimulus window passed through the straight ahead position. By drifting the visual stimuli across the screen, a laminar motion was added to the expansion pattern and shifted the focus of expansion on the retina in the exact same way as in the real pursuit condition. Between the real pursuit and simulated pursuit condition, the retinal image was identical; however, the difference was that in one condition, there was a real eye pursuit, while in the other, the pursuit was simulated with no actual eye movement.

Under examination, the tuning curves in the simulated pursuit condition aligned with the fixed gaze tuning curves when plotted in retinal coordinates, but not when plotted in screen coordinates. In this condition, the neuron was not able to compensate for the shift caused by drifting the visual stimuli across the screen. The finding that real pursuit was able to compensate for laminar motion, but simulated pursuit was not able to compensate, indicated that the extraretinal pursuit signal generated in the real pursuit condition was necessary for neurons in MSTd to shift their tuning curves to represent the true heading direction. In other words, the movement command was subtracted from the retinal image to recover the original location of the focus tuning curve in an extraretinal space. Bradley et al. found this extraretinal effect across the population of neurons recorded.

These results are in agreement with psychophysical studies. Humans are able to correctly report the heading direction in the real pursuit condition, but are not very accurate in the simulated pursuit condition (Royden et al., 1992; Royden et al., 1994). These results show that extraretinal pursuit eye movement signals are important in the accurate determination of heading direction. If the eye movement signal was not important, humans would also be able to determine the correct heading direction in the simulated pursuit condition since the retinal stimuli are identical in the pursuit and simulated pursuit conditions.

1.4.2 Head Rotation Compensation

The visual scene can be disturbed by head movements in addition to eye movements. Large gaze rotations typically involve both head movements and eye rotations. Psychophysical studies have shown that vestibular cues are necessary to accurately judge heading direction during head turns (Crowell et al., 1998). If area MSTd is involved in self-motion perception, then the neurons in this area should also be involved in compensation for the visual shift caused by head rotations, as they are for eye rotations (Bradley et al., 1996). Shenoy et al., (1999) recently investigated whether MSTd neurons can shift their tuning curves to compensate for head turns. In their experiments, instead of having the monkeys pursue a fixation point across an optic flow stimulus with eye movements, they had them perform vestibulo-ocular reflex cancellation (VORC). In the VORC condition, the monkey fixates on a target moving synchronously with the head and body while viewing an optic flow stimulus. The entire monkey is rotated, which generates vestibular cues. The eyes, head, and body do not move in relation to each other. In a different condition, the monkeys also made pursuit eye movements across the screen to directly compare the amount of compensation present between the eye pursuit and VORC conditions. Similar results were found across the population with 88% compensation for pursuit, and 77% for VORC (Shenoy et al., 1999). It appears that neurons in MSTd are receiving a vestibular signal in order to compensate in the VORC condition. This idea is supported by other studies that showed that many MSTd neurons are responsive to vestibular stimulation when monkeys are rotated in the dark (Thier and Erickson, 1992b).

This study also had a simulated pursuit condition where the retinal stimulus was drifted in the opposite direction of the gaze tracking tasks. The retinal stimulus was identical in both the VORC gaze tracking and simulated condition, the difference being the simulated condition did not generate any eye movement or vestibular cues. Interestingly, in the simulated pursuit condition, there was considerable compensation (52%). This indicated that both extraretinal and retinal factors contributed to the compensation. The Bradley et al., (1996) study did not find any compensation under the simulated pursuit condition. A potential explanation may be that a much larger stimulus was used in the Bradley study compared to Shenoy study. It is possible that the smaller display had more obvious edges when compared to the larger display and contributed to this compensation.

1.4.3 Pursuit Speed Compensation

As eye pursuit speed changes, the amount of shift in the retinal focus changes as well. A comparison of rows A and B of Figure 1-6 demonstrates how the focus of expansion shifts more for faster pursuit speeds. Psychophysical studies have shown that human subjects are able to compensate for changes in pursuit speed and correctly estimate heading direction over a wide range of eye pursuit speeds (Royden et al., 1992; Royden et al., 1994). If MSTd neurons are involved in self-motion perception, then they should be able to compensate for changes in pursuit speed as well. Due to the relationship of pursuit speed to the retinal focus shift for stimuli simulating approach to a frontoparallel wall, compensation should increase proportional to pursuit speed.

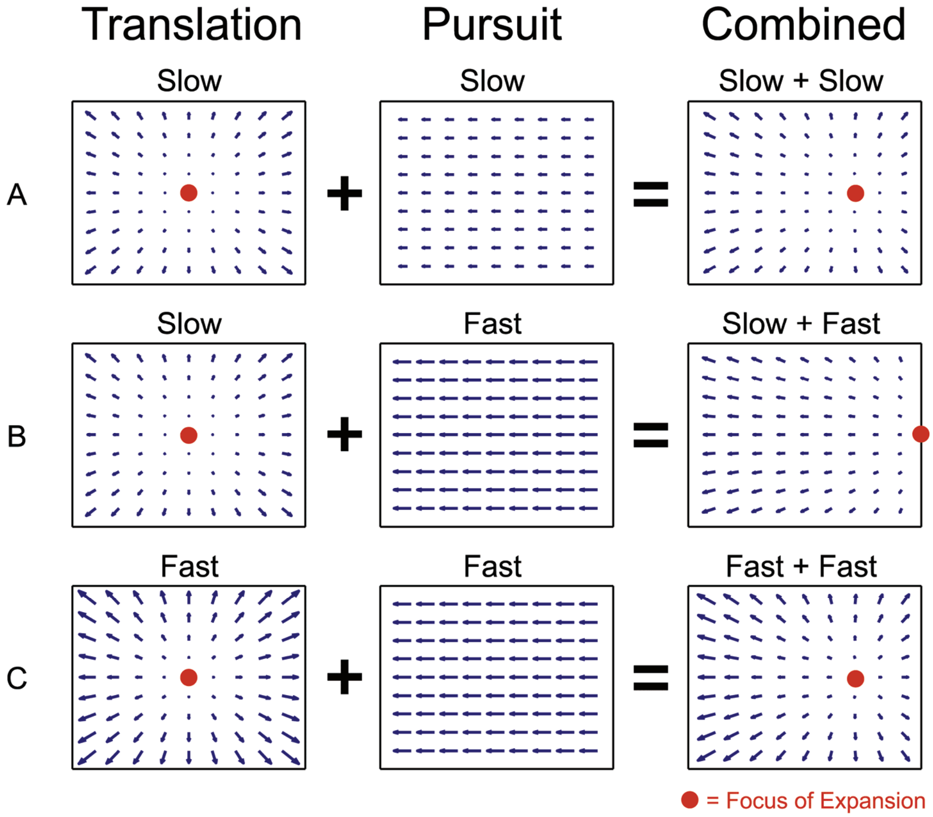

Figure 1-6 Schematic of Flow Fields on the Retina
Retinal motion patterns caused by observer translation and pursuit eye movements. Comparing row A to row B shows that the focus of expansion (FOE) shifts more on the retina for faster pursuit speeds than for slower pursuit speeds. The FOE shift is also affected by the speed of translation. This can be seen by comparing rows B and C. Note that although the pursuit speeds and translation speeds are different for row A and row C, the FOE location is the same.

Shenoy et al., (2002) found that MSTd neurons produced greater shifts in the focus tuning curves as pursuit speed increased, leading to the same percentage of compensation at different speeds. Figure 1-7 shows an example of an MSTd neuron tested with three different real and simulated pursuit speeds. The unity line represents 100% compensation, while the horizontal line corresponds to 0% compensation. Two regression lines were fit to the data for real and simulated pursuit. The slopes of the regression lines indicated this neuron was compensating by 66.9% for real pursuit and 34.8% for simulated pursuit. Across the population, the mean compensation was 55% for real pursuit and 42% for simulated pursuit.

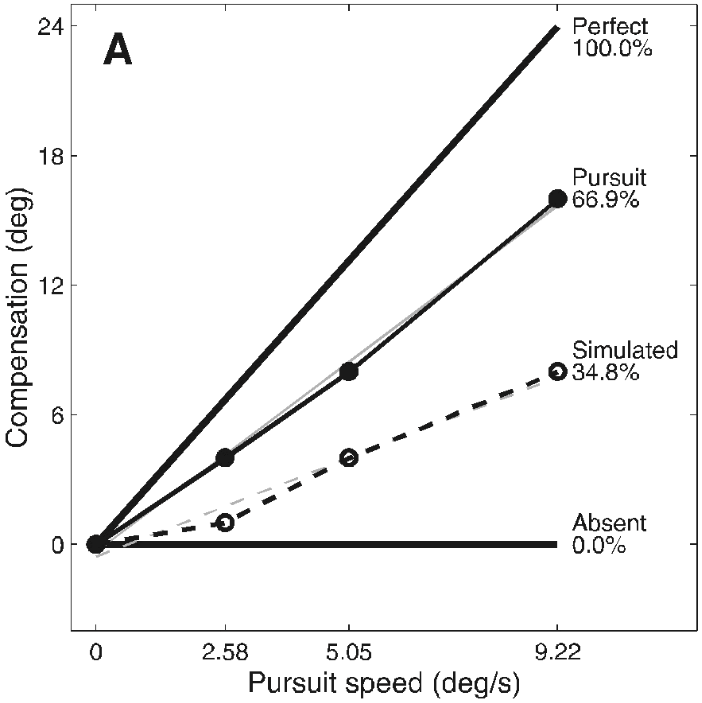

Figure 1-7 Compensatory Shift as a Function of Pursuit Speed
Accurate heading judgment requires more compensation during faster pursuit. 100% compensation is defined as the slope of perfect compensation versus pursuit speed curve, while the slope of the no compensation curve equals 0%. The real pursuit compensatory shifts are plotted as filled circles with solid lines. Simulated pursuit compensatory shifts are plotted as open circles with dashed lines. Lines were regressed to the real and simulated pursuit compensation curves and expressed the slopes as a percentage of the perfect compensation slope. This neuron exhibits 66.9% compensation for real pursuit and 34.8% for simulated pursuit. From Shenoy et al., (2002).

Since the amount of compensation increased in proportion to pursuit speed resulting in about the same compensation percentage over different pursuit speeds, this meant that eye rotation speed did not need to be represented in the template models. By not having to represent eye rotation speed in the template models, this significantly reduced the number of templates necessary to represent all possible flow patterns and made the template model more biologically plausible.

1.5 New Research

Building upon the body of knowledge that we have about area MSTd, we present our most recent experiments and their results, which help us better understand the role of this brain area in heading perception.

1.5.1 Translation Speed Compensation

The focus of expansion is determined by both eye pursuit speed and observer translation speed. Previous research has already shown that neurons in MSTd can compensate for changes in eye pursuit speed (Shenoy et al., 2002). But can MSTd neurons compensate for changes in translation speed? The shift in the focus of expansion (FOE) is affected by the speed of translation, which can be seen by comparing rows B and C in Figure 1-6 Due to the inverse relationship between the focus of expansion and the speed of translation, faster translation causes less of a shift in the FOE than slower translation. In Chapter 2 we will examine whether neurons in MSTd can compensate for changes in translation speed during pursuit eye movements. If MSTd neurons can compensate for changes in translation speed, this would indicate that neurons in this cortical area are able to use retinal information in the stimulus to compute compensation. We will also investigate whether MSTd neurons can correctly compensate for visual stimuli that vary both translation speed and pursuit speed at the same time. If the neurons are able to do this, then it is possible that the retinal factor of translation speed and extraretinal factor of eye pursuit are handled by the same set of templates, further reducing the number of templates and neurons required for heading computation.

1.5.2 Coordinate Frame

In the early parts of the visual system, the visual signals generated by self-motion are represented in retinal coordinates. Since this information can be used to navigate the observer through the environment, it must be transformed into body or world coordinates at the later stations of the visual-motor pathway. It is not known in which coordinate frame MSTd neurons represent heading direction. In Chapter 3 we will examine whether neurons in MSTd represent heading in eye, head, body, or world coordinates. These different coordinate frames can be separated by recording focus tuning curves from different eye positions for testing eye-centered coordinates, head positions for testing head-centered coordinates, body positions with respect to the head for testing body-centered coordinates, and orientations of the entire animal in the room for testing world-centered coordinates. Since the visual information in area MSTd can be used for navigation, it is possible that the signals are already represented in body or world coordinates. However, many neighboring areas in the posterior parietal area represent their respective modalities in an eye-centered reference frame. In addition, we will explore the possibility that MSTd neurons represent their focus tuning curves in different coordinate frames when the eyes are stationary compared to when they are moving. Finally, any eye position gain modulation will be examined as well.

Chapter 2: Translation Speed Compensation in Cortical Area MSTd

2.1 Introduction

The goal of this study is to understand how the neurons in the dorsal aspect of the medial superior temporal area (MSTd) compute heading direction from optic flow. It has been previously proposed that for an individual in motion, the focus of expansion (FOE) of the retinal image could be used to determine the direction of heading (Gibson, 1950). However, when eye and head movements are present, the focus of expansion no longer corresponds with heading direction (Longuet-Higgins and Prazdny, 1980; Koenderink and van Doorn, 1986). To appreciate this, imagine an observer walking down the road while their eyes are fixating on an airplane flying across the horizon from left to right. As the observer moves forward and follows the moving plane with their eyes, the eyes rotate in the head. This eye movement adds a laminar motion to the forward translation component of the visual field that is in the opposite direction of the eye movement. As a result, the retinal focus of expansion is shifted in the direction of eye movement and no longer indicates the true heading direction. Figure 2-1A

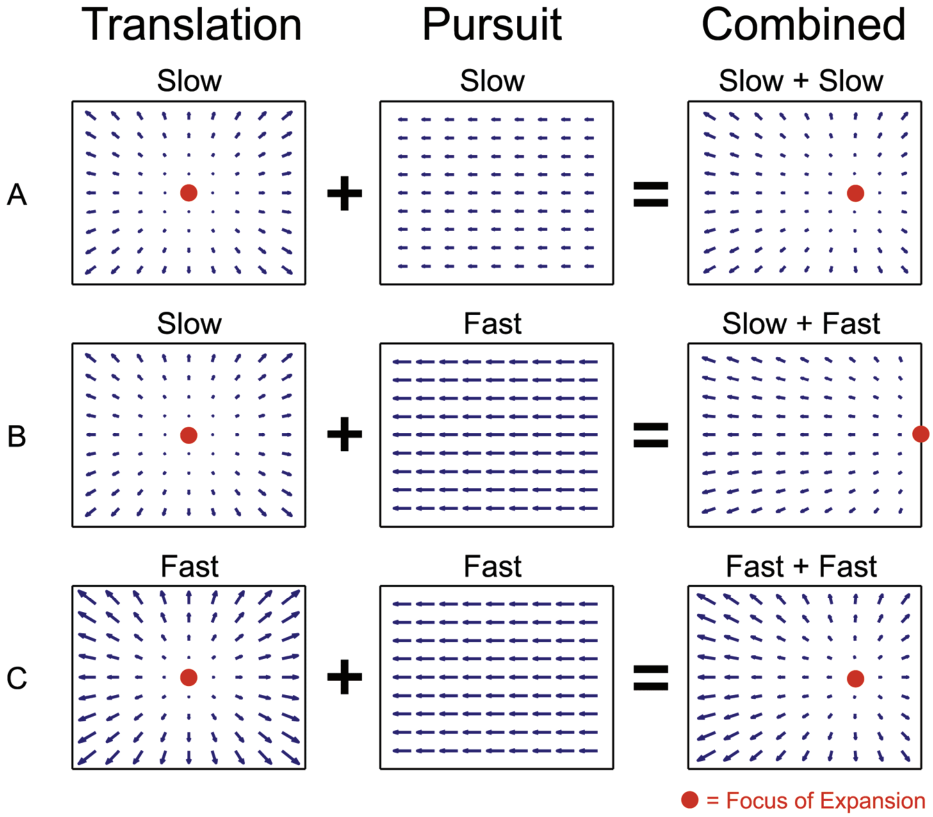

Figure 2-1 Schematic of Flow Fields on the Retina
Retinal motion patterns caused by observer translation and pursuit eye movements. Comparing row A to row B shows that the focus of expansion (FOE) shifts more on the retina for faster pursuit speeds than for slower pursuit speeds. The FOE shift is also affected by the speed of translation. This can be seen by comparing rows B and C. Note that although the pursuit speeds and translation speeds are different for row A and row C, the FOE location is the same.

MSTd neurons have many properties that suggests they are involved in self-motion processing such as large receptive fields, selectivity for optic flow patterns (Komatsu and Wurtz, 1988b, a; Duffy and Wurtz, 1991b, a; Graziano et al., 1994; Lagae et al., 1994), tuning for the retinal position of the FOE (Duffy and Wurtz, 1995), and tuning for the rate of expansion (Duffy and Wurtz, 1997).

Research from our laboratory has found that neurons in MSTd adjust their focus tuning in response to the laminar motion produced by eye rotations, thereby recovering the true focus of expansion, which corresponds to the true heading direction (Bradley et al., 1996; Shenoy et al., 1999). Since the focus of expansion shifts more on the retina for faster pursuit speeds, greater focus tuning compensation is required as pursuit speed increases. In line with this, MSTd neurons have been shown to adjust their focus tuning in accordance with changes in eye pursuit speed (Shenoy et al., 2002).

The translation speed of an observer also affects the shift of the focus of expansion. This can be seen by comparing rows B and C in Figure 2-1. Faster translation causes the focus of expansion to shift less on the retina than slower translation. If MSTd neurons are involved in self-motion perception, then they should demonstrate varying compensation as translation speed changes. We recorded neural responses from 93 MSTd neurons as monkeys were presented with optic flow stimuli simulating a range of 11 heading directions. The forward translation was simulated at three different translation speeds while the monkeys were required to fixate or pursue across the display. This experimental paradigm allowed us to examine the effects of varying the translation speed for a given pursuit speed. The results we report here indicate that area MSTd does in fact compensate for changes in translation speed, which suggests it combines retinal cues related to translation speed with extraretinal signals related to eye movements to compute heading direction.

2.2 Materials and Methods

The methods described in this section have been previously reported (Shenoy et al., 1999; Shenoy et al., 2002). We will briefly review them here.

2.2.1 Animal Preparation

The Caltech Institutional Animal Care and Use Committee approved all protocols. We recorded extracellular responses from 93 MSTd neurons in two rhesus monkeys (*Macaca mulatta*). Both monkeys were naïve to the experimental paradigm. We implanted bone screws into the skull upon which a methylmethacrylate head cap was built. This head cap featured a titanium head post that allowed the monkey's head to be immobilized. In monkey DON a scleral search coil was implanted between the conjunctiva and sclera and used to monitor eye position at 1000 Hz (Judge et al., 1980). The search coil was connected to a coaxial connector located on the methylmethacrylate head cap. For monkey ROY, we used an optical eye tracker to monitor eye position at 240 Hz (ISCAN, Burlington, MA). Behavioral training commenced approximately one week after surgery. During training, the monkeys were given a juice reward for correctly performing each trial. After several weeks of training, performance levels reached above 90%. At this time, we performed a second surgery to open a craniotomy and implanted a surface-normal chronic recording chamber. The recording chamber was located at 5 mm posterior, 17 mm lateral, on the right hemisphere in both DON and ROY.

2.2.2 Recording Techniques

We recorded extracellular action potentials with glass-coated tungsten microelectrodes with impedances between 1.0-1.5 MΩ (Alpha-Omega, Nazareth, Israel). Through the chronic recording chamber, a stainless steel guide tube was manually advanced through the dura and then the electrode was further lowered into the cortex via an FHC hydraulic microdrive (FHC, Bowdoinham, ME). The electrode was advanced until neurons could be heard. At this point, the electrode was allowed to settle for 30 minutes. MSTd neurons were identified by stereotaxic coordinates, MRI anatomical images, depth in the chamber, position relative to other cortical areas, and response properties such as optic flow tuning and large receptive fields that were both ipsilateral and contralateral. Only optic flow tuned neurons were recorded and included in our analysis. Neural data was sampled at 20,000 Hz and recorded and analyzed with custom software. All experiments were performed in an acoustically and radio frequency shielded room.

2.2.3 Visual Stimuli

The monkeys performed all the tasks in complete darkness, except for the visual stimuli. The visual stimulus was displayed on a high-resolution flat screen CRT monitor at a resolution of 800 x 600 and frame rate of 120 Hz. This monitor was placed 38.1 cm from the eyes of the monkey and filled 57° x 45° of the visual field. The stimulus was 20° x 20° in size and contained 400 stimulus dots. The dots were white (10 candela/m^2) on a black background and anti-aliased for smooth movement. Each dot was given an age between 0 to 287 ms and traveled at a constant velocity until 300 ms expired, or until it crossed the edge of the stimulus window, in which case it was moved to a new random position in the stimulus. The speed of the stimulus dots increased in proportion to the distance from the focus of expansion. Both monkeys viewed the stimulus monocularly with the left eye to eliminate stereo cues. Stimulus dots were 2.5 x 2.5 pixels in size while fixation points were larger at 5 x 5 pixels.

2.2.4 Behavioral Tasks

After the electrode was allowed to settle in the cortex for 30 minutes, we began to isolate single neurons. Once a neuron was isolated, we mapped out the receptive field by displaying an expansion optic flow stimulus at different positions on the screen. The center of the stimulus was tested at 0°,0°; +5°,+5°; +5°,–5°; –5°,–5°; and –5°,+5° with respect to the fixation point, which was always located at 0°,0°. The position with the strongest response to the expansion stimuli was then used for all subsequent experiments. We first ran three sets of characterization tasks to determine the preferred spiral space pattern, the preferred laminar motion, and the preferred pursuit direction. After the neuron was characterized, we then ran the translation speed compensation task.

2.2.4.1 Characterization Tasks

2.2.4.1.1 Preferred Spiral Space Pattern

After the receptive field was determined, we displayed eight spiral space patterns to measure the selectivity of each neuron. Spiral space includes expansions, contractions, rotations, and their combinations. These visual patterns are generated on the retina during self-motion toward and away from a frontoparallel plane, as well as during self-rotation about the axis of heading. Activity in spiral space can be represented in two dimensions with expansions/contractions represented along the horizontal axis and rotations along the vertical.

Spiral space is constructed by rotating the motion vectors in an expansion stimulus by different counterclockwise angles: 0° for expansion, 45° for a counterclockwise-expanding spiral, 90° for counterclockwise rotation, 135° for a counterclockwise-contracting spiral, 180° for contraction, 225° for a clockwise-contracting spiral, 270° for clockwise rotation, and 315° for a clockwise-expanding spiral. The neuron's preferred spiral space pattern can be seen by plotting the tuning curves in spiral space. The tuning curves for MSTd neurons in response to spiral space stimuli are typically single-peaked and smoothly varying (Graziano et al., 1994; Geesaman and Andersen, 1996). Since we are interested in exploring whether MSTd neurons can compensate for changes in translation speed due to forward motion, we searched for neurons that were most responsive to spiral space patterns that contained an expansion component.

2.2.4.1.2 *Preferred Laminar Motion*

We also determined the laminar motion tuning of each neuron, since laminar motion tuning is an identifying characteristic of area MSTd. Laminar motions are generated on the retina during lateral self-motion. They are also generated during eye and head rotations. We used the laminar motion task to estimate the response of MSTd neurons to purely visual laminar motion in the absence of either self-motion or eye and head movements. The laminar motion stimuli consisted of random dots moving unidirectionally in one of eight directions, spaced at 45° apart.

Other than differences in the visual stimuli, both the preferred spiral space pattern and preferred laminar motion tasks used the same behavioral task. At the beginning of each trial, a fixation point appeared on the screen and the monkey was required to fixate within 800 ms otherwise the trial would abort. Fixation was required to be maintained within a ± 2° window around the fixation point until the end of the trial. Once the monkey obtained fixation, the optic flow pattern was displayed for 1200 ms resulting in a total trial duration of 2000 ms. The last 1000 ms of this period was used to measure the activity of the neuron. By discarding the first 200 ms of the period in which the optic flow pattern was displayed, we avoided the phasic response to the onset of the stimuli and only analyzed the tonic response. Overall, we ran three trials per condition to determine the mean rate of activity. Three trials per condition has proven sufficient to measure the neuron's response, yet the number of trials was low enough that all the conditions can be tested in a single recording session (Shenoy et al., 2002).

2.2.4.1.3 Preferred Pursuit Direction

In this block of trials, we determined the preferred pursuit direction of each MSTd neuron. Spiral space and laminar motion stimuli involve purely retinal cues while pursuit eye movements also involve extraretinal signals related to the eye movement itself. These extraretinal signals may reflect the eye movement command or efference copy, from other brain areas. We used the pursuit task to quantify the extent to which extraretinal signals are represented in area MSTd. In this task, the monkey pursued in eight directions spaced 45° apart to determine the neuron's preferred pursuit direction. This preferred direction was noted and used in the translation compensation task.

The preferred pursuit direction was determined by having the monkey pursue a small white dot on a black background with no other visual stimuli on the screen. Since MSTd neural firing rates increase with increasing pursuit speeds, we used a rather fast pursuit speed of 8°/s to elicit a large neural response (Shenoy et al., 1999; Shenoy et al., 2002). We tested eight pursuit directions spaced 45° apart. Within 800 ms of the stimulus appearance, the monkey was required to obtain and maintain fixation inside a ± 2° moving window that surrounded the moving fixation point. The fixation point continued to move for an additional 1200 ms for a total trial duration of 2000 ms. To remove gaze angle effects, pursuit trajectories were centered around the straight ahead (0°,0°) location on the monitor.

2.2.4.2 Translation Speed Compensation

In this block of trials, we examined the effects of different speeds of translation and pursuit on compensation in three randomly interleaved conditions: fixed gaze, real pursuit, and simulated pursuit. Figure 2-2 The heading stimuli consisted of an expansion flow field with the foci positioned at 11 locations in 6° steps (range ± 30°) along the preferred axis of pursuit as determined earlier. Since the stimulus window was 20° x 20° and always located at the same position on the screen, the FOE would sometimes be outside the window, but the centrifugal dots from the expansion pattern were always visible within this window.

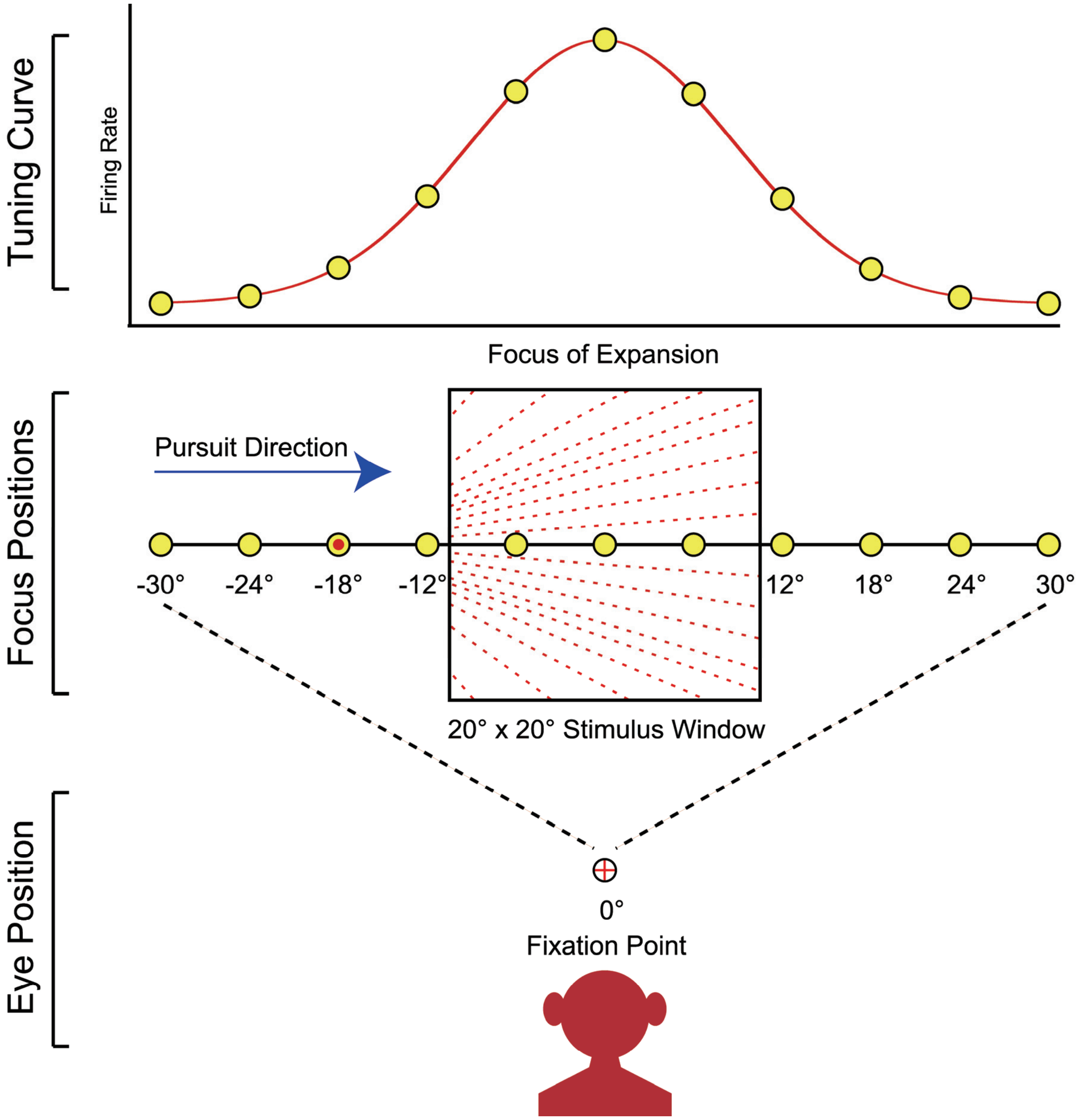

Figure 2-2 Translation Speed Task Diagram
The monkey was required to fixate at 0°,0°. The heading stimuli consisted of an expansion flow field with the foci positioned at 11 locations in 6° steps (range ± 30°) along the preferred axis of pursuit. The activity at the 11 FOE locations was used to generate a tuning curve. The stimulus window was 20° x 20° in size and contained 400 dots. Since the stimulus window was always located at the same position on the screen, the FOE would sometimes be outside the window, but the centrifugal dots from the expansion pattern were always visible within this window (shown in figure). In the fixed gaze condition, the monkey simply maintained fixation on a static fixation point. In the real pursuit condition, the monkey pursued a moving fixation point across the stimulus window. In the simulated pursuit condition, the monkey fixated at a static fixation point and the entire stimulus was drifted across the screen at the same speed, but in the opposite direction as in the real pursuit condition.

In the fixed gaze condition, the stimulus was presented on the monitor as the monkey fixated on a stationary fixation point. Since there was no eye movement in this condition, the visual image and retinal image were identical and represented the actual direction of heading. In the real pursuit condition, the stimulus was again presented at a fixed location on the monitor; however, the monkey was required to pursue a moving fixation point across the stimulus window. The moving fixation point traveled in the preferred direction of the neuron as determined earlier. This eye movement caused the focus of expansion to shift on the retina. As a result, the focus of expansion no longer represented the direction of heading. In the simulated pursuit condition, the retinal image was identical to the retinal image in the real pursuit condition. This was accomplished in the simulated pursuit condition by drifting the entire stimulus across the screen at the same speed, but in the opposite direction as in the real pursuit condition to ensure that all aspects of the retinal stimulus were identical in the two conditions. Of the three conditions, only the retinal image in the fixed gaze condition accurately represented the direction of heading. The real and simulated pursuit conditions both had shifted focus of expansions that no longer represented the direction of heading. The difference between the real and simulated pursuit conditions was that the eyes actually moved in the real pursuit condition, but not in the simulated pursuit condition.

For both the real pursuit and simulated pursuit conditions, we used three different (real and simulated) pursuit speeds (2.5, 5.0, and 8.0°/s) and three different simulated translation speeds (10, 16, 20 cm/s). Table 2-1 Since there was no pursuit in the fixed gaze condition, we only varied the three translation speeds. This gave us a total of 21 conditions (3 fixed gaze + 9 real pursuit + 9 simulated pursuit). The different pursuit speeds at different translation speeds produced focus shifts ranging from 4.8° to 30.5°.

Translation \ Pursuit	2.5°/s	5.0°/s	8.0 °/s
10 cm/s	9.53°	19.05°	30.48°
16 cm/s	5.95°	11.9°	19.05°
20 cm/s	4.76°	9.53°	15.24°

Table 2-1 Focus of Expansion Shifts
In the real pursuit and simulated pursuit conditions, the focus of expansion was shifted on the retina by combining three pursuit speeds and three translation speeds.

2.2.5 Data Analysis

2.2.5.1 Preferred Spiral Space Pattern, Preferred Laminar Motion, and Preferred Pursuit Direction

We calculated the preferred spiral space pattern and preferred laminar motion directions by plotting tuning curves in spiral and laminar space and computing the response weighted vector sum (Geesaman and Andersen, 1996; Shenoy et al., 1999; Shenoy et al., 2002). The preferred pursuit direction was also determined using this technique. A significant modulation of activity by direction was measured by using the Rayleigh test (Geesaman and Andersen, 1996; Zar, 1996).

2.2.5.2 Translation and Pursuit Compensation

The governing equation of the retinal image when approaching a frontoparallel wall is

$$\frac{dx}{dt} = \frac{T_z}{z} x \quad \text{(Equation 2-1)}$$

Where:

$x =$ distance of a point on the wall from the center

$dx/dt =$ radial speed

$T_z =$ translation speed

$z =$ distance from the wall

To determine the retinal location of the focus of expansion during smooth pursuit eye movements, we set dx/dt as the pursuit speed and solve Equation 2-1 for x:

$$x = \frac{dx}{dt} \frac{1}{T_z} z \quad \text{(Equation 2-2)}$$

This equation shows how the location of focus x changes as a function of the pursuit and translation speed. The value of z in Equation 2-2 is the distance of the monkey's eyes to the monitor and is fixed at 38.1 cm. The retinal location of the focus of expansion depends linearly on pursuit speed (dx/dt) and hyperbolically on translation speed ($1/T_z$).

We chose pursuit speeds between 0 and 10°/s due to constraints of the monitor size. Also, faster pursuit is more difficult for the monkeys to perform. Similarly, translation speed was constrained between 10 and 20 cm/s so that we didn't encounter translation/pursuit speed combinations where pursuit speed had little effect on focus shift (T_z > 20 cm/s) or a large effect on focus shift (T_z < 10 cm/s).

2.2.5.3 Cross-correlation

Compensation is calculated by measuring the horizontal shift of the tuning curves obtained in the real and simulated pursuit conditions with respect to the tuning curve measured in the fixed gaze condition. We calculated the cross-correlation coefficient at each 6° step of the 11 FOE locations along the pursuit axis (Bradley et al., 1996; Shenoy et al., 1999; Shenoy et al., 2002). Cross-correlation is well-suited for this type of well-sampled data due to its sensitivity to the horizontal alignment of tuning curves regardless of their exact functional form. In addition, it is insensitive to any vertical shifts or gain changes between the curves that may be present. One potential drawback of using cross-correlation is that the range of shifts tested must be restricted to avoid computing cross-correlations where there are not enough overlapping points. We avoided this problem by designing the analysis such that of the 11 focus positions, there were always 6 or more overlapping sample points.

To interpolate between the 6° measures, the tuning curves were spline interpolated with 1° sampling. In previous studies, we found that the results are similar without such smoothing (Shenoy et al., 1999; Shenoy et al., 2002). However, using spline interpolation allows us to detect small shifts. The shift that produces the highest correlation coefficient was used to compute the compensation. Compensation was defined as the difference between the theoretical shift of the focus on the retina and the measured shift using cross-correlation, divided by the theoretical shift. Percent compensation was calculated by multiplying this term by 100. For example, if the theoretical retinal shift during a pursuit condition was 12°, and the actual shift was only 3°, then the compensation is (12° – 3°)/12° = 0.75, and the percent compensation is 75%.

2.2.5.4 ANOVA

To examine the effects of pursuit speed and translation speed on compensation in area MSTd, we performed a 2-way ANOVA on the 3 x 3 array of compensations. A significant result for pursuit speed or translation speed would indicate that the compensation was not uniform but depended on one of the factors. We then explored if the two factors were combined independently or if there was an interaction between them by examining the interaction term from the ANOVA.

2.2.5.5 Regression analysis

To further quantify the effects of translation and pursuit speed we performed a regression analysis on the measured shifts of the tuning curves. Since we know the association between the retinal shifts, pursuit speed, and translation speed (Equation 2-2), we can estimate how well the compensation follows this relationship. We first examined simplified versions of Equation 2-2 by regressing single variable models using pursuit or translation speed alone. The goodness of fit of the regressions indicated how well these single variable models represented the data. We then fit the complete model of Equation 2-2 and examined the significance of fit. A significant improvement in the fit would suggest that the neurons are doing the appropriate calculations and the two factors are interacting as predicted by Equation 2-2.

2.3 RESULTS

We recorded neural activity from 93 neurons in two monkeys, 64 from monkey DON and 29 from monkey ROY. All neurons were first characterized in the spiral space, laminar motion, and pursuit tasks and then tested in the translation speed compensation tasks. Neurons were selected for having significant responses for all three conditions of fixed gaze, real pursuit, and simulated pursuit at a translation speed of 16 cm/s and pursuit speed of 8°/s. These parameters were chosen to allow comparison with previous experiments in our laboratory.

2.3.1 Characterization Tasks

2.3.1.1 Spiral Space Tuning

Across the population, 86/93 (93%) neurons recorded were significantly tuned to one direction in spiral space ($p<0.05$, Rayleigh test). Figure 2-3A Most of the neurons showed the greatest response to an optic flow pattern that contained an expansion component 82/93 (88%) neurons. The preferred response across the population of neurons was $-11° \pm 10°$ (95% confidence interval) and the distribution was not uniform ($p<0.05$, Rayleigh test). Since we specifically searched for neurons that were responsive to expansion flow patterns, this distribution may not be reflective of the overall representation of spiral space patterns in MSTd.

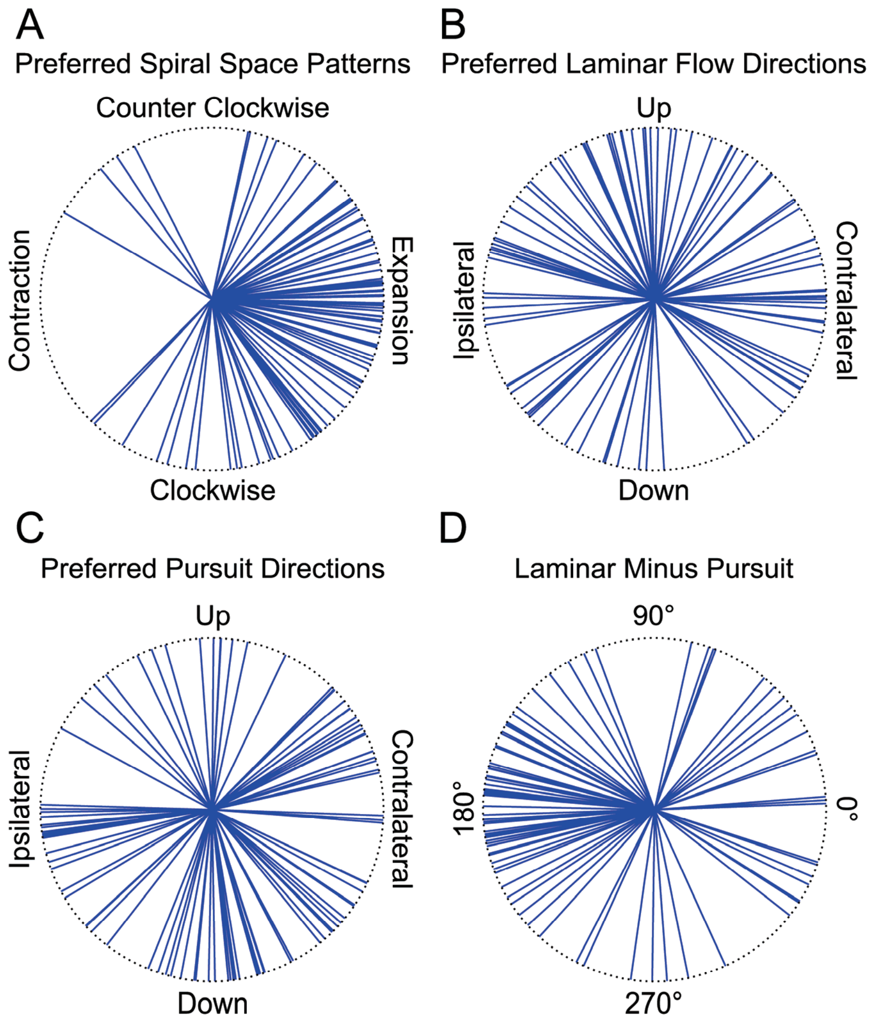

Figure 2-3 Population: Spiral / Laminar / Pursuit / Anti-alignment
A. Spiral space: 86/93 (93%) neurons recorded were significantly tuned to one direction in spiral space ($p<0.05$, Rayleigh test). The preferred response across the population of neurons was –11° ± 10° (95% confidence interval) and the distribution was not uniform ($p<0.05$, Rayleigh test). Most of the neurons showed the greatest response to an optic flow pattern that contained an expansion component 82/93 (88%) neurons.

B. Laminar: 80/93 (86%) MSTd neurons showed significant tuning to laminar motion stimuli ($p<0.05$, Rayleigh test). The distribution of preferred directions was not uniform and was slightly biased towards upward motion ($p<0.05$, Rayleigh test). There was a slight ipsilateral bias: 50/93 (54%) neurons.

C. Pursuit: 76/93 (82%) MSTd neurons showed significant tuning to pursuit ($p<0.05$, Rayleigh test). The distribution of preferred pursuit directions was not uniform and was slightly biased towards downward motion ($p<0.05$, Rayleigh test). There was a slight contralateral bias: 56/93 (60%) neurons.

D. Anti-alignment of laminar and pursuit tuning: On a population level, laminar and pursuit tuning showed an anti-alignment of 178° ± 14° (95% confidence interval) and the distribution was not uniform ($p<0.05$, Rayleigh test). Most neurons had an anti-alignment between 90° and 270°: 67/93 (72%) neurons.

2.3.1.2 Laminar Tuning

80/93 (86%) MSTd neurons showed significant tuning to laminar motion stimuli ($p<0.05$, Rayleigh test). Figure 2-3B The distribution of preferred directions was not uniform and was biased towards upward motion ($p<0.05$, Rayleigh test). There was also a slight ipsilateral bias: 50/93 (54%) neurons.

2.3.1.3 Pursuit Tuning

76/93 (82%) MSTd neurons showed significant tuning to pursuit ($p<0.05$, Rayleigh test). Figure 2-3C The distribution of preferred pursuit directions was not uniform and was biased toward downward motion ($p<0.05$, Rayleigh test). There was also a contralateral bias: 56/93 (60%) neurons.

2.3.1.4 Anti-alignment of Laminar and Pursuit Tuning

On a population level, laminar and pursuit tuning showed an anti-alignment of $178° \pm 14°$ (95% confidence interval) with a non-uniform distribution ($p<0.05$, Rayleigh test). Most neurons had an anti-alignment between 90° and 270°: 67/93 (72%) neurons. Figure 2-3D Laminar tuning is exclusively retinal while pursuit tuning is reflective of an extraretinal eye movement signal. It is possible that neurons in MSTd extract retinal information from laminar motion and combine it with extraretinal pursuit activity to compute heading direction. This is consistent with previous reports (Sakata et al., 1978, 1983; Komatsu and Wurtz, 1988a; Shenoy et al., 2002).

2.3.2 Translation / Pursuit Speed Compensation

2.3.2.1 Single Neuron Compensation

Computing heading direction involves compensating for eye movements by subtracting their influence from the optic flow pattern. After determining the axis of preferred pursuit, we tested how well MSTd neurons compensate for pursuit eye movements by orienting the focus of expansion stimuli along the axis of preferred pursuit. Figure 2-4 shows the response of an example neuron to these stimuli at three different translation speeds and three different pursuit speeds. For this neuron, the simulated headings (FOE) were situated from –30° to +30° in 6° increments along the vertical axis (90°). We will explain in detail the tuning of this neuron using the middle panel in the top row of Figure 2-4 (TS=10 cm/s, PS=5.0°/s). The fixed gaze tuning curve (blue solid) peaks around –18° to –24° and is the neural response to the focus of expansion at the 11 points spanning –30° to +30°. Since the eyes were not moving, the focus position on the retina corresponds to the true heading in this fixed gaze condition.

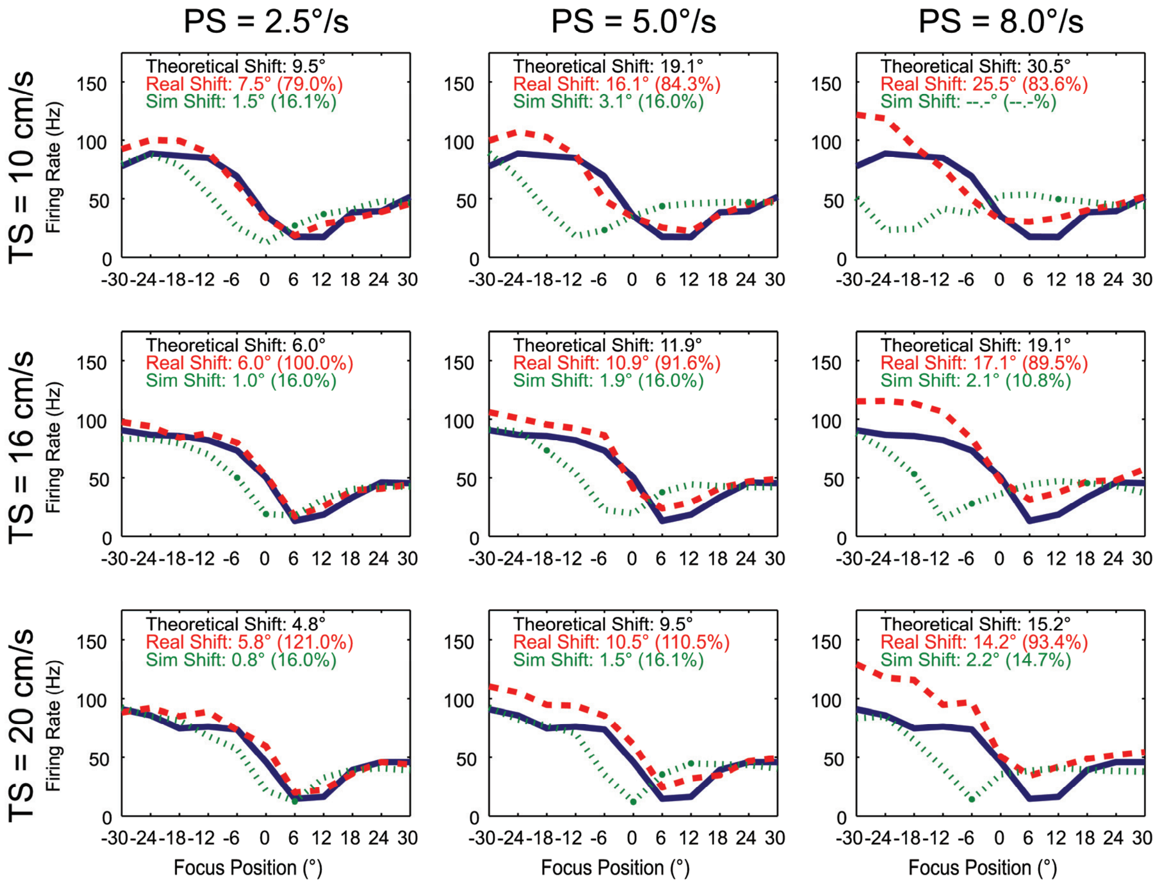

Figure 2-4 Single Neuron Compensation: 3 Translation Speeds x 3 Pursuit Speeds
Tuning curves and calculated compensations of an example neuron at three translation speeds and three pursuit speeds. Simulated headings (FOE) were situated from –30° to +30° in 6° increments along the vertical axis (90°). Fixed gaze tuning curves: blue solid line; real pursuit: red dashed line; and simulated pursuit: green dotted line. Since the eyes were not moving, the focus position on the retina corresponded to the true heading in the fixed gaze condition. Theoretical shift is the amount the real and simulated pursuit condition tuning curves would need to shift for perfect (100%) compensation. Horizontal shifts were calculated using cross-correlation. For the TS=10 cm/s, PS=8.0°/s condition, the simulated pursuit compensation could not be calculated because the tuning curve features were too far apart and resulted in an erroneous calculation.

In the real pursuit condition, the eye movement caused a shift of the focus of expansion on the retina in the same direction as the pursuit, in our example, 19.1°. If this neuron were simply reporting the focus position on the retina, then we would expect the focus tuning curve to move downwards by 19.1° or left along the x-axis. On the other hand, if this neuron were reporting the perceived heading direction, then the focus tuning curve would not shift on our plot, even though the image on the retina was shifted. In this case, the neuron would be compensating for the shift of the focus of expansion caused by eye movements by shifting its tuning curve to represent the perceived heading direction and not the actual image on the retina. A third possibility is the neuron had an incomplete shift somewhere between the true heading and retinal image. This would occur if the neuron were computing perceived heading direction but did not shift its focus tuning curve far enough to represent the true heading direction.

In our example neuron, for the real pursuit condition (red dashed), the focus tuning curve is close to the focus tuning curve during fixation (fixed gaze; solid blue), indicating that this neuron is reporting the approximate true heading instead of the retinal image. In order to quantify how much shift actually occurred, we cross-correlated the fixed gaze and real pursuit tuning curves. The maximum correlation coefficient is found at an offset of (3°). If this neuron were simply reporting the location of the retinal image, there would be a shift of 19.1°. A value of 3° tells us that this neuron was almost fully compensating for the effect of pursuit eye movements and was shifting its tuning curves to represent true heading. Using our compensation index formula, we calculate that this neuron compensates by 16.1°/19.1° = 0.843 or 84.3%.

We next asked whether this neuron shifted its tuning curves in the simulated pursuit condition when there were only retinal cues present and no actual eye movements. Again, using cross-correlation we find that the simulated pursuit tuning curve (green dotted) is 16.0° away from the fixed gaze focus tuning curve. It is very close to the tuning curve representing the retinal image, not the direction of heading. This neuron shows 3.1°/19.1° = 0.16 or 16% compensation. In the simulated pursuit condition, this neuron shows significantly less compensation than in the real pursuit condition indicating that the actual pursuit eye movement is important in heading computation. However, the compensation value for the simulated pursuit condition is not zero, which demonstrates that MSTd neurons can use purely retinal cues to shift the focus tuning curve towards the fixed gaze tuning curve (true heading).

Since we know that MSTd neurons can partially compensate for simulated pursuit, which is based upon retinal information and not actual eye movement or efference copy, we asked whether MSTd neurons can adjust their tuning curves to changes in translation speed that are also only based upon retinal input. In the middle column of Figure 2-4, the pursuit speed was kept the same (5.0°/s), however the translation speed changed from 10 to 16 to 20 cm/s. In this manner we were able to keep pursuit speed the same and examine the effects of varying the translation speed.

By inspection, it is apparent that the real pursuit tuning curves are very close to the fixed gaze tuning curves for all three translation speeds. When the actual shift is calculated for the real pursuit condition, this MSTd neuron shifted its tuning curves to compensate for eye movements by 16.1° to 10.9° to 10.5° as translation speed increased. Since there is an inverse relationship between translation speed and the shift of the focus of expansion, increases in translation speed result in smaller focus of expansion shifts. The real pursuit tuning curves align closely to the fixed gaze tuning curves (true heading). This means that neurons in MSTd were able to use purely retinal information related to translation speed to shift their tuning curves towards true heading. The pursuit speeds in the three conditions were identical so the changes in the tuning curves are due to retinal information alone.

Since this effect is based on purely retinal information, we would expect the simulated pursuit condition, which does not have any eye movement component and only has retinal information, to also compensate for changes in translation speed. We found this is the case. The tuning curves shift from 3.1° to 1.9° to 1.5° as translation speed increased. While this is not enough for full compensation to represent true heading, it shows that the retinal information alone can be used by neurons in MSTd to partially compensate and shift their tuning curves towards the true heading direction.

2.3.2.2 Translation Speed Compensation: Single Neuron Example

To examine a single neuron's response across varying translation and pursuit speeds, we plotted the compensation as a function of the inverse of translation speed in the real pursuit and simulated pursuit conditions. Figure 2-5 shows the results of translation speed compensation for the example neuron. The thick blue line represents 100% compensation while 0% compensation would be represented by a perfectly horizontal line. The dashed red line is real pursuit and the dotted green line is simulated pursuit. Compensation increased as 1/(translation speed) increased for both the real and simulated pursuit conditions. To calculate the compensation percentage, we regressed lines (thin black lines) through the real and simulated translation data. When translation speed becomes large enough, the value of 1/(translation speed) approaches zero so we included this point in our regression. Intuitively, we can understand this effect by visualizing the movement of dots in the visual stimuli as we increase translation speed. With high translation speed, the dots of the visual stimuli move towards you much more than they move across the screen. Therefore, increasing translation speed compresses the horizontal shift due to pursuit movements. We calculated the compensation index for the regression lines by dividing each regression line by the slope of the perfect compensation line. For this neuron, at a pursuit speed of 2.5°/s, real pursuit resulted in 57% compensation and simulated pursuit resulted in 35% compensation. While some neurons increased their compensation in direct proportion to 1/(translation speed), most neurons did not display a linear dependence.

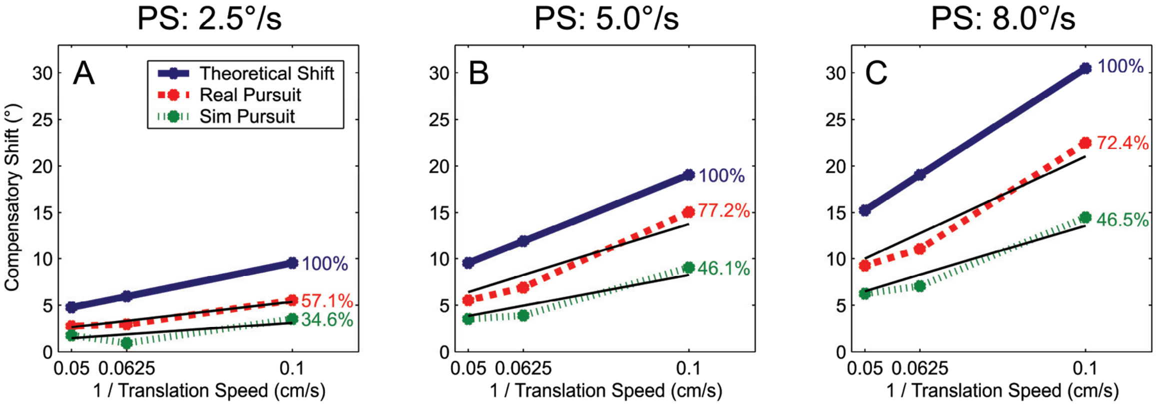

Figure 2-5 Single Neuron: Translation Speed Compensation
Compensation is plotted as a function of the inverse of translation speed in the real pursuit and simulated pursuit conditions. The thick blue line represents 100% compensation. 0% compensation would be represented by a perfectly horizontal line. The dashed red line is real pursuit and the dotted green line is simulated pursuit. The thin black lines are regressions through the real and simulated pursuit conditions. We calculated the compensation percentage from the regression lines by dividing each regression line by the slope of the perfect compensation line. While some neurons increased their compensation in direct proportion to 1/(translation speed), most neurons did not display a linear dependence. We averaged the regression lines across all three pursuit speeds to generate a single compensation percentage for both real and simulated pursuit. On the whole, this neuron compensated 69% for real pursuit and 42% for simulated pursuit.

For both the real and simulated pursuit conditions, the slopes were positive indicating that compensation increased as 1/(translation speed) increased. The slope for the real pursuit condition was also greater than the slope for the simulated pursuit condition which means that real pursuit results in greater compensation compared to simulated pursuit.

We averaged the regression lines across all three pursuit speeds to generate a single compensation percentage for both real and simulated pursuit. On the whole, this neuron compensated 69% for real pursuit and 42% for simulated pursuit.

2.3.2.3 Translation Speed Compensation: Population

Here we calculated and plotted the mean population compensation shift during real and simulated pursuit as a function of 1/(translation speed). Figure 2-6 We regressed lines through the mean compensations for both real and simulated pursuit. Error bars are 95% confidence intervals. On a population level, there was greater compensation as 1/(translation speed) increased. There was also greater compensation for real pursuit compared to simulated pursuit. For the population, the average compensation across all pursuit speeds was 70% for real pursuit and 36% for simulated pursuit.

While most individual neurons did not display a linear dependence of compensation with 1/(translation speed), across the population of MSTd neurons, we found that the compensation increased with 1/(translation speed) in a linear manner. This is advantageous from a computational standpoint: regardless of the translation speed, the percent compensation would remain the same because of the linear dependence of compensation on translation speed.

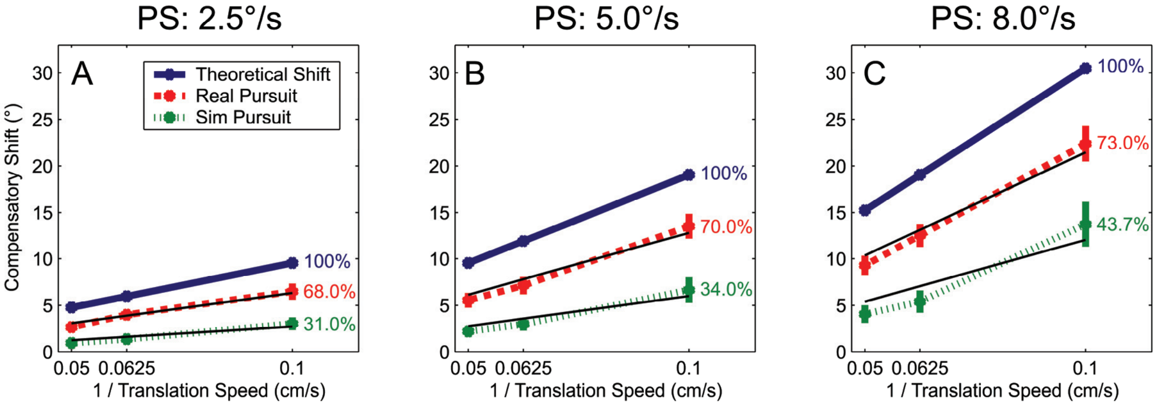

Figure 2-6 Population: Translation Speed Compensation
Plots of the mean population compensation shift during real and simulated pursuit as a function of 1/(translation speed). Error bars are 95% confidence intervals. For the population, the average compensation across all pursuit speeds was 70% for real pursuit and 36% for simulated pursuit. While most individual neurons did not display a linear dependence on 1/(translation speed), across the population of MSTd neurons, we found that the compensation increased with 1/(translation speed) in a roughly linear manner.

2.3.2.4 Pursuit Speed Compensation: Population

In addition to translation speed compensation, we also examined the pursuit speed compensation of our population and compared the results with previous studies from our laboratory. Figure 2-7 We plotted our population data with respect to increasing pursuit speed for a fixed translation speed, in essence repeating the experiments of Shenoy et al., (2002). Our results are in line with theirs. Under similar conditions, at a translation speed of 16 cm/s, we found 65% compensation during real pursuit and 28% compensation during simulated pursuit. Shenoy et al., (2002) calculated 55% and 42%, respectively. Across all the conditions, we found 66% compensation during real pursuit and 33% compensation during simulated pursuit.

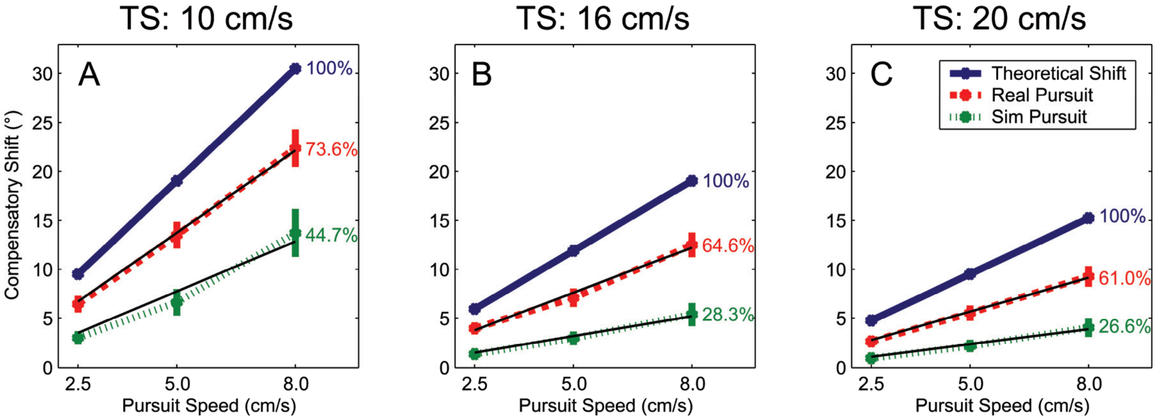

Figure 2-7 Population: Pursuit Speed Compensation
Plots of the mean population compensation shift during real and simulated pursuit as a function of pursuit speed. We included the 0° compensation at 0°/s pursuit speed data point in the regression. For the population, the average compensation across all pursuit speeds was 66% for real pursuit and 33% for simulated pursuit. Across the population of MSTd neurons, we found that the compensation increased with pursuit speed in a roughly linear manner.

2.3.2.5 Compensation Comparisons for FOE Shifts of the Same Value

In the translation speed experiment, three translation speeds were tiled with three pursuit speeds. Of the nine FOE shifts, there were two sets of replicates, namely 9.53° and 19.05° Table 2-2A The 9.53° focus shift arises from TS=10/PS=2.5 and TS=20/PS=5, while the 19.05° shift is the result of TS=10/PS=5 and TS=16/PS=8. Although these two sets of FOE shifts have the same value, they arrive from different translation speed and pursuit speed combinations. This is essentially comparing rows A and C in Figure 2-1. We can compare the amount of compensation within each pair to see if the compensation is the same. If neurons in MSTd only used extraretinal signals, i.e. pursuit speed, then the compensation would be different when comparing the two variants for each FOE shift. However, if MSTd neurons use both extraretinal and retinal signals due to translation speed, then the compensation for both variants of each FOE shift should be similar.

A.

Translation \ Pursuit	2.5°/s	5.0°/s	8.0 °/s
10 cm/s	9.53°	19.05°	30.48°
16 cm/s	5.95°	11.9°	19.05°
20 cm/s	4.76°	9.53°	15.24°

B.

Theoretical Shift	Pursuit	Translation Speed	Pursuit Speed	Calculated Shift	t-test
9.53°	Real	10 cm/s	2.5°/s	6.5°	Same
		20 cm/s	5.0°/s	5.5°	
	Simulated	10 cm/s	2.5°/s	3.0°	Same
		20 cm/s	5.0°/s	2.2°	
19.05°	Real	10 cm/s	5.0°/s	13.5°	Same
		16 cm/s	8.0°/s	12.5°	
	Simulated	10 cm/s	5.0°/s	6.6°	Same
		16 cm/s	8.0°/s	5.4°	

Table 2-2 Focus Shifts for 9.53° and 19.05° for Different PS/TS Values
A. Of the nine tested focus of expansion shifts, there are two sets of replicates, 9.53° (TS=10/PS=2.5 and TS=20/PS=5) and 19.05° (TS=10/PS=5 and TS=16/PS=8). These two sets of FOE shifts, although they are the same, arrive from different translation speed and pursuit speeds combinations. This is essentially comparing rows A and C in Figure 2-1.

B. A t-test was run to compare the compensation within each pair of FOE shifts and found that the compensation was the same at the p=0.05 level. This was true in both the real and simulated pursuit conditions.

We ran a t-test on the means for each pair of FOE shifts and found that the means were the same ($p<0.05$, t-test). Table 2-2B This shows that neurons in MSTd used both retinal and extraretinal cues in computing heading direction during translation. MSTd neurons were able to shift their focus tuning curves to represent true heading in response to changes in both translation speed and pursuit speed.

2.3.2.6 ANOVA

To analyze the effects of pursuit speed and translation speed we performed a 2-way ANOVA on the 3 x 3 array of compensations. Table 2-3A A significant result for one factor or another would suggest that the compensation is affected by pursuit speed and/or translation speed. The interaction term from the ANOVA indicates whether the two factors are combined independently or if there is an interaction between them.

We found that translation speed is significant in 76/93 (82%) of neurons during real pursuit and 64/93 (69%) of neurons during simulated pursuit. The similarity between the number of neurons that are significant for translation speed in the real and simulated pursuit condition is expected since translation speed is a retinal cue that is identical in both conditions. This result demonstrates that translation speed is used by area MSTd to compute heading.

Pursuit speed is significant in 86/93 (93%) of neurons during real pursuit and 58/93 (62%) of neurons during simulated pursuit. The difference in the number of neurons that are significant to pursuit speed may be because during real pursuit, there is an actual eye movement while in simulated pursuit, the eye is stationary and the stimulus is dragged across the visual field in order to simulate eye pursuit. It appears that the actual eye movement in the real pursuit condition recruits a larger number of neurons when calculating the translation and pursuit speed.

There is a significant interaction effect in 36/93 (39%) of neurons during real pursuit and 34/93 (37%) of neurons during simulated pursuit. A significant interaction effect means that pursuit speed and translation speed are interacting in a non-linear manner.

A. ANOVA		
	Real Pursuit	Simulated Pursuit
Translation Speed effect	76 (81.7%)	64 (68.8%)
Pursuit Speed effect	86 (92.5%)	58 (62.4%)
Interaction effect	36 (38.7%)	34 (36.6%)

B. Regression		
	Real	Simulated
1/(Translation Speed) * 38.1	5 (5.4%)	13 (14.0%)
Pursuit Speed * 38.1	13 (14.0%)	20 (21.5%)
Pursuit Speed / (Translation Speed) * 38.1	54 (58.1%)	50 (53.8%)

Total Neurons: 93

Table 2-3 Population: ANOVA / Regressions
A: Number of neurons significant in a 2-way ANOVA for the factors of translation speed, pursuit speed, and the interaction of translation speed and pursuit speed.

B: Regression analysis on the measured shifts of the tuning curves for a single variable model of FOE = 1/(Translation Speed) * 38.1, single variable model of FOE = Pursuit Speed * 38.1, and the complete model of FOE = Pursuit Speed / Translation Speed * 38.1. 38.1 is the distance of the monkey's eyes to the monitor in centimeters.

2.3.2.7 Regression

To understand the relationship between translation and pursuit speed we performed a regression analysis on the measured shifts of the tuning curves. Table 2-3B Assuming the functional dependency of the retinal shifts on pursuit speed and translation speed is similar to Equation 2-2, we can estimate how well the compensation follows this relationship. We first regressed single variable models (pursuit or translation speed alone) using simplified versions of Equation 2-2. We then fit the full model given by Equation 2-2 and assessed the significance of the fit. A significant improvement in the fit would suggest that the two factors interact in the way predicted by Equation 2-2; i.e., the neurons are doing the appropriate calculations.

We first regressed the measured shift of the focus of expansion tuning curves to the single variable model of FOE = 1/(translation speed) * 38.1. We found that only 5 (5%) neurons during real pursuit and 13 (14%) of neurons during simulated pursuit had a significant fit to this model. Similarly, when we regressed the single variable model of FOE = pursuit speed * 38.1 we found that only 13 (14%) of neurons during real pursuit and 20 (22%) of neurons during simulated pursuit demonstrated a significant fit. This regression analysis shows that the computation does not functionally follow FOE = 1/(translation speed) * 38.1 only or FOE = pursuit speed * 38.1 only.

However, when we regress the compensation shifts to the full model of FOE = PS / TS * 38.1, we find 54/93 (58%) and 50/93 (54%) of neurons demonstrate a significant fit for real pursuit and simulated pursuit, respectively. This indicates that many MSTd neurons are doing calculations in accordance with Equation 2-2.

2.4 Discussion

We examined whether neurons in MSTd are able to shift their tuning curves towards the actual direction of heading in order to compensate for the shift of the FOE brought about by changes in translation speed. The neurons were first tested for their optic flow preferences as well as for preferred pursuit direction. Consistent with previous studies, we found that MSTd neurons are selective to spiral space patterns, especially for those that have an expansion component (Duffy and Wurtz, 1991b, a; Orban et al., 1992; Graziano et al., 1994; Sakata et al., 1994). However, it must be noted that in our study, we specifically looked for neurons that had expansion tuning, so the proportion of neurons we report as having expansion tuning is likely higher than those reported in other studies. The majority of neurons in MSTd show significant tuning to laminar motion; however, we did not find a contralateral visual motion bias that others have reported (Komatsu and Wurtz, 1988b; Shenoy et al., 2002). We found that most MSTd neurons show significant pursuit activity as reported in other studies (Kawano et al., 1984; Komatsu and Wurtz, 1988b; Erickson and Thier, 1991; Bradley et al., 1996; Shenoy et al., 2002). The distribution of preferred directions was not uniform as there was a slight bias towards the contralateral side. This contralateral preference was seen in other studies as well (Komatsu and Wurtz, 1988b).

We also found an anti-correlation between preferred laminar motion and preferred pursuit direction. This combination of extraretinal information and purely retinal information may be necessary for visual processing and heading determination. Laminar and pursuit integration might be explained by a mechanism discovered by Sakata et al., (1978, 1983) and further explored by Komatsu and Wurtz (1988b). When pursuing an object across the visual scene, the background moves in the opposite direction of the eye movement. If area MSTd is integrating laminar motion with pursuit eye movements, then one would expect a higher firing rate when pursuing across a static background versus pursuing across a background without any salient features. Komatsu and Wurtz found that MSTd neurons do enhance their firing rate when pursuing across a visible background compared to pursuit in the dark (Komatsu and Wurtz, 1988b). This mechanism integrates retinal and extraretinal signals together and can be a basis of compensation.

We found that individual MSTd neurons are able to shift their tuning curves to compensate for changes in translation speed. This was true in both the real and simulated pursuit conditions. While some neurons increased their compensation in direct proportion to 1/(translation speed), most neurons did not display a linear dependence. However, across the population of MSTd neurons, the compensation increased with 1/(translation speed) in a roughly linear manner. Shenoy et al., (2002) also found this property of MSTd when examining pursuit speed compensation. In their study, as they increased pursuit speed, individual MSTd neurons also increased their compensation, although the increase was not in direct proportion to pursuit speed and the response was not linear. However, their entire population did show a roughly linear increase in compensatory shift as a function of pursuit speed. This population level linear dependence for compensation with varying translation speed and pursuit speed simplifies computation for an area that is downstream of MSTd receiving heading information. In this manner, regardless of the translation and pursuit speed, neurons in MSTd compensated for the shifted FOE due to eye pursuit by the same amount. In our translation speed experiment, we find that amount to be approximately 70% when the eyes are making a real pursuit movement and 36% for simulated pursuit regardless of translation and pursuit speed.

While there is much psychophysical and physiological evidence that an extraretinal signal is important in pursuit compensation, several computational papers have hypothesized that under the correct conditions, there is enough information in the pattern of retinal motion for the visual system to estimate translation and rotation components without an extraretinal signal (Longuet-Higgins and Prazdny, 1980; Rieger and Lawton, 1985; Heeger and Jepson, 1992; Perrone and Stone, 1994; Lappe et al., 1996). However, experimental human studies have contradicted this idea and shown that human subjects are rather poor at judging their direction of self-motion when shown simulated pursuit heading stimuli (Royden et al., 1992; Royden, 1994; Banks et al., 1996; Crowell et al., 1998). In fact, studies by Crowell et al. found 0% compensation during the simulated pursuit condition (Crowell et al., 1998b; Crowell and Andersen, 2001).

We used similar experimental setups as the studies discussed above, and, on the contrary, we found significant compensation effects in the simulated pursuit condition. The MSTd neurons compensate about equally for the 1/(translation speed) regression (36% in Figure 2-6) and for the pursuit speed regression (33% Figure 2-7). It is possible that differences in the physiological and psychophysical results may be explained by the size of the stimuli. In our study, the stimulus occupied a 20° x 20° window while in the human psychophysical studies, the stimulus occupied a 40° x 40° window. The issue of the stimulus size and its effectiveness in driving retinal-based compensation has been a subject of debate in the literature. Koenderink and van Doorn (1987) showed that simulated pursuit compensation is possible if the scene has a large field of view and contains depth variation. A single frontoparallel plane stimulus, like the one in this present study, would not provide enough information to compute self-motion accurately. Supporting this claim for compensation requiring large stimuli are psychophysical studies that demonstrate accurate self-motion judgments during simulated pursuit using large displays (90° x 90°), while performance was not accurate with smaller displays (Grigo and Lappe, 1999).

Our physiological results disagree with the idea that larger stimuli are needed for retinal-based compensation. Bradley et al. found in their neurophysiology experiments that large stimuli (50° x 50° and up) are less effective in driving retinal-based compensation in the simulated pursuit condition (Bradley et al., 1996), when compared to smaller stimuli (20° x 20°). Our results support small size stimuli as being more effective in generating compensation in the simulated pursuit condition. A possible explanation lies in the fact that smaller stimuli have more salient borders, which could improve compensation. According to this, the large stimuli would have their borders positioned in the periphery of the visual field, therefore reducing any possible compensatory effects.

In this current study, we find that retinal as well as extraretinal signals are combined to shift FOE tuning curves in order to represent the heading direction in MSTd. It should be noted that the same FOE shifts may correspond to different translation speed / pursuit speed combinations. The regression analysis showed that many neurons in MSTd are shifting their focus tuning curves according to Equation 2-2. This is significant in that both translation speed and pursuit speed are represented in Equation 2-2. However since we did not observe 100% compensation for either real or simulated pursuit, it is possible that area MSTd is doing a calculation that is similar to but not exactly like Equation 2-2, or the calculations are being done at a lower gain.

In summary, the results presented here indicate that many neurons in MSTd shift their focus tuning curves to adjust for changes in translation speed. Previous work in our laboratory has shown that MSTd neurons can shift their tuning curves to adjust for eye movements (Bradley et al., 1996) and changes in pursuit speed (Shenoy et al., 2002). These results combined with our finding that MSTd neurons can compensate for changes in translation speed further support the idea that MSTd is an important cortical area in self-motion processing.

Chapter 3: Area MSTd Represents Heading in an Eye-Centered Coordinate Frame

3.1 Introduction

As we move through the environment, the visual image expands on our retinas. Gibson suggested that humans can use the point from which the visual image expands, the focus of expansion (FOE), to determine the direction of self-motion (Gibson, 1950). A region of the brain that is involved in the perception of self-motion is the dorsal aspect of the medial superior temporal area (MSTd).

Neurons in MSTd are sensitive to optic flow, which can theoretically be used for navigation. Studies have found that MSTd neurons are able to shift their tuning curves to compensate for visual perturbations caused by eye movements in order to represent the direction of heading as opposed to representing the retinal image (Bradley et al., 1996). In addition, MSTd neurons are able to compensate for changes in pursuit speeds (Shenoy et al., 2002). Recently our laboratory has shown that MSTd neurons can also compensate for changes in translation speed. (See Chapter 2) This gives strong support to the idea that MSTd is involved in heading computation.

However, it is not known in which coordinate frame neurons in MSTd represent heading direction. Self-motion generates visual signals that are initially represented in retinal coordinates as the image is captured on the retina. This visual information is later transformed into body or world coordinates so the information can be used to navigate the observer through the environment. Since optic flow is necessary for navigation, MSTd neurons could be coding in body or world coordinates. These different coordinate frames can be teased apart by collecting focus tuning curves from various eye positions (for testing eye-centered coordinates), head positions (for testing head-centered coordinates), body positions with respect to the head (for testing body-centered coordinates), and orientations of the entire animal in the room (for testing world-centered coordinates).

The finding that area MSTd represents self-motion in eye coordinates would be consistent with neighboring cortical areas. Many other areas of the posterior parietal cortex compensate for eye movements in an eye-centered coordinate frame. For example, activity related to the remembered locations of saccade targets is updated in eye coordinates for intervening saccades (Gnadt and Andersen, 1988; Duhamel et al., 1992). The parietal reach region codes the location of reach targets in eye coordinates, and similarly compensates for intervening saccades (Batista et al., 1999). The advantage of a common coordinate frame for movement representations is that the target locations can then be transformed into other coordinate frames at later stages of the nervous system using eye, head, and body position signals (Andersen, 1997; Cohen and Andersen, 2002).

If we find that MSTd neurons are coding in eye-centered coordinates, we will then investigate how the neural activity is modulated by eye position. Many other posterior parietal areas exhibit eye and head position gain effects where the response fields are otherwise in eye coordinates (Andersen et al., 1997). Previous studies have shown that this modulation can be the basis of a distributed code for head-centered and body-centered coordinates (Zipser and Andersen, 1988; Pouget and Sejnowski, 1995; Xing and Andersen, 2000).

3.2 Materials and methods

3.2.1 Animal Preparation, Recording Techniques, Visual Stimuli

Please refer to Section 2.2.1 through 2.2.3 for details on animal preparation, recording techniques, and visual stimuli.

3.2.2 Behavioral Tasks

3.2.2.1 Characterization Tasks

Please refer to Section 2.2.4.1.1 through 2.2.4.1.3 for details on how we determined the preferred spiral space pattern, preferred laminar motion, and preferred pursuit direction.

3.2.2.2 Coordinate Frame Task

In this block of experiments, we determined whether the focus tuning curves in MSTd were represented in eye, head, body, or world coordinates. We first ran experiments to determine if MSTd neurons were coding in eye coordinates versus screen coordinates. Screen coordinates refers to any downstream coordinate frame other than the one that is explicitly being tested. In this case, screen coordinates refers to any coordinate frame other than eye coordinates, i.e., head, body, world. If the results indicated that neurons MSTd were coding in eye coordinates, we would not need to continue testing the other coordinate frames. However, if the results indicated screen coordinates, we would test for head coordinates versus screen coordinates (body and world). This would continue until a definitive coordinate frame was determined.

We first started by comparing eye coordinates and screen coordinates. The first set of trials was performed to determine the coordinate frame with the eyes stationary while the second set was performed to determine the coordinate frame during pursuit eye movements. A third set of trials was performed to test the coordinate frame of MSTd neurons during a simulated pursuit condition.

The heading stimuli were displayed in a 20° x 20° window centered at 0°,0° with respect to the eye. Figure 3-1 The stimuli consisted of an expansion flow field with the foci located at 11 points in 6° steps (range ± 30°) along the previously determined preferred axis of pursuit. Although the FOE would sometimes be outside the stimulus window, the centrifugal dots from the expansion pattern were always visible inside this window. In the fixed gaze condition, the monkey’s eyes were stationary and fixed on a fixation point. In the real pursuit condition, the moving fixation point traveled in the direction of preferred pursuit across the stimulus window. In the simulated pursuit condition, the eyes were stationary and the entire stimulus was drifted across the screen in the opposite direction and at the same speed as in the real pursuit condition. In this manner, all aspects of the retinal image were identical in the real pursuit and simulated pursuit condition.

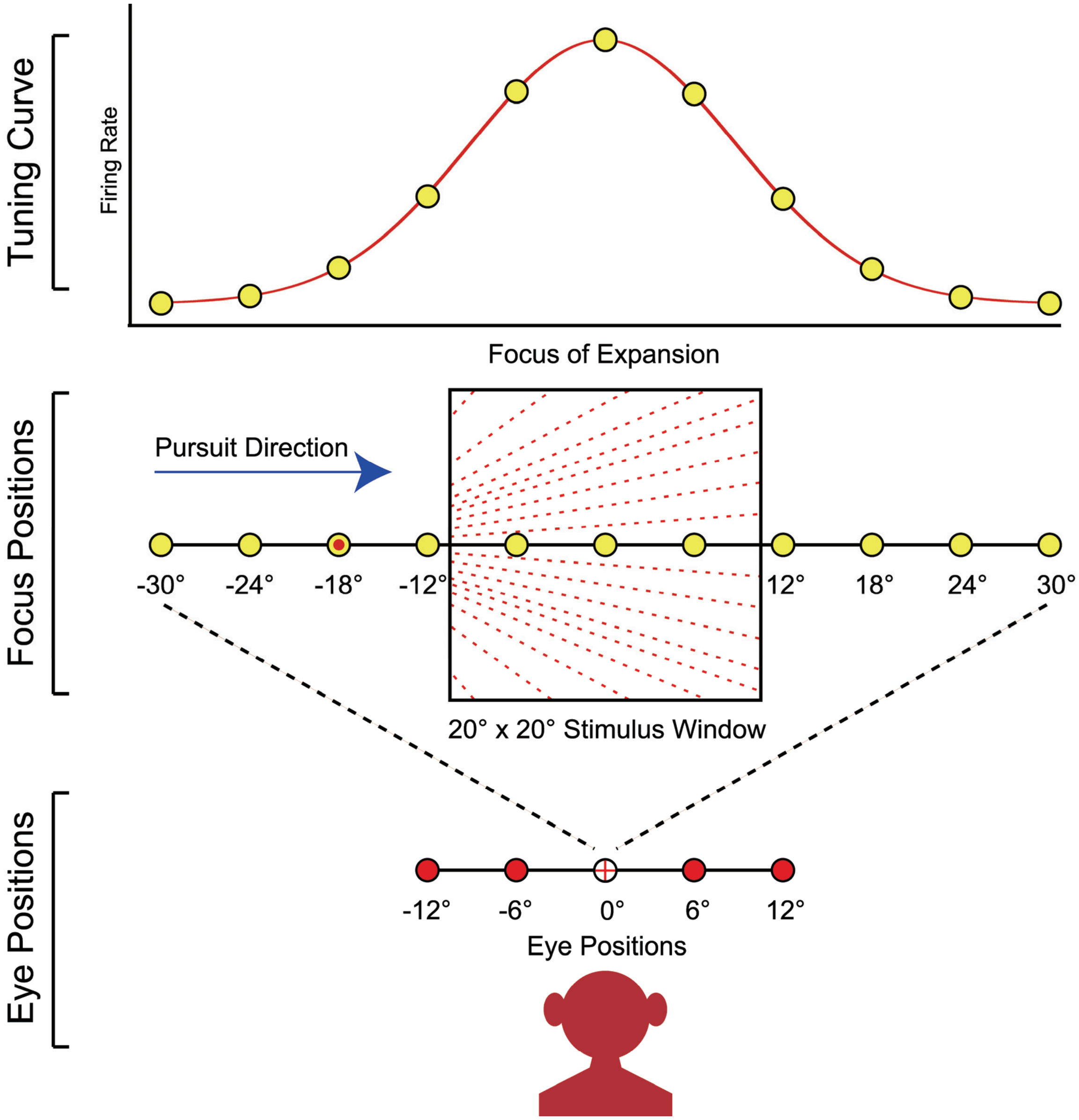

Figure 3-1 Coordinate Frame Task Diagram
The monkey was required to fixate within a ± 2° window surrounding five possible fixation points (5 x 5 pixels) oriented along the preferred axis of pursuit separated by 6° steps (range ± 24°). The heading stimuli was displayed in a 20°x20° window centered at 0°,0° with respect to the eye. The stimuli consisted of an expansion flow field with the foci located at 11 points in 6° steps (range ± 30°) along the previously determined preferred axis of pursuit. Although the FOE would sometimes be outside the stimulus window, the centrifugal dots from the expansion pattern were always visible inside this window. (Shown in figure.)

In the fixed gaze condition, the monkey simply maintained fixation on one of the five fixation points. In the real pursuit condition, the monkey pursued a moving fixation point across the stationary stimulus window. In the simulated pursuit condition, the retinal image was identical to the real pursuit condition by having the monkey fixate at a stationary fixation point and drifting the entire stimulus across the screen in the opposite direction and same speed as in the real pursuit condition. In both the real and simulated pursuit conditions, pursuit was performed along the horizontal plane and also along the diagonals; however, due to screen size limitations, pursuit was not performed on the vertical axis.

3.2.2.2.1 Coordinate Frame Testing with Eyes Stationary

The first set of experiments examined the coordinate frame of MSTd expansion tuning curves when the eyes were stationary. The focus tuning was determined at five eye positions from –12° to +12° in 6° increments along the axis of preferred pursuit. Due to screen size constraints, the vertical pursuit directions (90° and 270°) were not used and the nearest 45° diagonal was substituted. The stimulus was presented in the same relative position to the eye for each eye position so that the retinal image remained the same across eye positions. An expansion pattern simulating a forward translation speed of 16 cm/s was used. The monkey was required to obtain fixation on the target (± 2° window) within 800 ms and remain fixated for an additional 1200 ms that the stimulus was presented. The total trial length was 2000 ms. The tuning curves were plotted in screen and eye coordinates. If the neurons were coding in eye coordinates, then the focus tuning curves would best align in that coordinate frame. However, if the tuning curves aligned in screen coordinates, then the tuning curves were in a non-retinal coordinate frame such as head, body, or world coordinates.

3.2.2.2.2 Coordinate Frame Testing During Real and Simulated Pursuit

This next set of experiments examined the coordinate frame of MSTd neurons during real and simulated eye pursuit. This experiment was similar to the one above, but added pursuit and simulated pursuit conditions. In the real pursuit condition, the monkey pursued the fixation point, which moved across the visual stimuli at 8°/s along the preferred axis of pursuit. The retinal image was identical in the simulated pursuit and the real pursuit condition. This was accomplished in the simulated pursuit condition by having the monkey fixate on the screen and then drifting the entire stimulus across the visual field in the opposite direction and at the same speed as in the real pursuit condition. Again, the tuning curves would be most aligned in the coordinate frame in which they were best represented.

3.2.3 Data Analysis

3.2.3.1 Preferred Spiral Space Pattern, Preferred Laminar Motion, and Preferred Pursuit Direction

Please refer to Chapter 2 for details on how we determined the preferred flow pattern, preferred laminar motion, and preferred pursuit direction.

3.2.3.2 Coordinate Frame

Previous studies demonstrated that posterior parietal areas, including MSTd, do not vary their preferred directions with changes in eye position (Andersen et al., 1990; Bremmer et al., 1997). This allowed us to compare the tuning curves at each eye position without having to worry about changes in preferred tuning, which could introduce bias into the results.

All analyses were performed with respect to the eye, which means the five fixation points were collapsed into a single point and the focus tuning curves were compared to each other. If area MSTd were coding in eye coordinates, the focus tuning curves would move with the eye and when the eye positions were overlaid onto the same point, all the tuning curves would overlap each other closely and there would be little or no horizontal shift between them. However, if neurons in MSTd were coding in screen coordinates (any other coordinate frame other than eye-centered), the focus tuning curves would stay at the same position on the screen regardless of eye position and when the eye positions were overlaid onto the same point, all the tuning curves would be misaligned by 6°, which is the distance between the eye positions.

We calculated the shift between the focus tuning curves measured at eye position 1 (–12°) and eye position 5 (+12°) which are the most distant eye positions and span 24°. The fixation points were overlaid on top of each other and if area MSTd is coding in eye coordinates, the measured shift between the two curves would be ~0°. If MSTd neurons are coding in screen coordinates, the measured shift would be ~24°.

We used cross-correlation to measure the amount of shift between the tuning curves. Cross-correlation works well for this type of well-sampled data because it indicates the horizontal shift between tuning curves and is insensitive to any vertical shifts or gain changes that may be present. To avoid calculating cross-correlations where there were not enough overlapping points, we constructed the analysis such that there were always six or more overlapping FOE locations. In order to detect small shifts, we first interpolated between the 6° FOE points with 1° spline interpolation (Shenoy et al., 1999; Shenoy et al., 2002). We then calculated the cross-correlation coefficient at each 1° step.

The shift that produced the highest correlation coefficient was used to calculate the amount of shift (Bradley et al., 1996; Shenoy et al., 1999; Shenoy et al., 2002).

3.2.3.3 Shift Index

In order to calculate the coordinate frame of the population, we created a shift index where 0 = eye coordinates and 1 = screen coordinates. We took the calculated shift between eye position 1 and eye position 5 and divided this by the actual distance between eye position 1 and eye position 5, which is 24°. This index would give an indication whether area MSTd were coding in eye coordinates, screen coordinates, or somewhere in between.

3.2.3.4 Singular Value Decomposition

In order to test whether there was a multiplicative interaction between eye position and focus of expansion tuning curves, we performed a singular value decomposition (SVD) on the matrix of responses where eye position and focus of expansion were varied. The SVD determines how well eye positions can be separated from focus of expansion tuning curves by multiplication (Pena and Konishi, 2001). This was done by modeling the responses as a weighted sum of matrices each of which multiplies the eye position and the focus of expansion tuning curves. If the response was separable as a gain field, the response energy was primarily concentrated in the first singular value and a multiplicative model was a good fit. However, if the response was vectorial, a multiplicative model was not a good fit and a gain field was not separable. In this scenario, the response energy would be strong in singular values other than just the first singular value.

A mean value was subtracted from the response matrix before performing the SVD. Separability was defined by a significantly ($p<0.05$) large first singular value when compared to the first singular value of randomized trial conditions (Randomization test). In our analysis, we classified the responses as separable or inseparable according to the $p=0.05$ threshold instead of by the strength of separability, which is defined by the magnitude of the first singular value compared with the others.

A multiplicative interaction would result if there was an eye position gain field modulation of responses. For responses that showed a multiplicative interaction the SVD estimated the shape of the average tuning curve and gain field.

3.2.3.5 Gain Analysis

Once the gain fields were calculated from the SVD analysis, we analyzed the gain fields. The gain fields were fit by a linear model and then linear regression techniques were used to partition the variability into the components of residual “pure error” and “lack of fit” (Kleinbaum and Kupper, 1978; Neter et al., 1983; Draper and Smith, 1998). The sum-of-squares lack-of-fit was the difference between the sum-of-squares of the model data and the sum-of-squares of the pure error. The F statistic was the ratio of mean-square lack-of-fit divided by the mean-square pure error. A p-value could then be calculated from the F statistic.

Our analysis separated the gain fields into four categories (Andersen et al., 1990). Neurons that had significant planar components ($p<0.05$) and no significant lack-of-fit ($p > 0.05$) were classified as planar (P). These types of gain fields were best fit by a planar model. Neurons that had a significant planar component ($p<0.05$) but also had a significant lack-of-fit ($p<0.05$) were classified as planar component (PC). A simple planar model fit part of the gain fields, but could not account for all of the variance. No planar component (NO) gain fields had no significant planar component ($p > 0.05$) but did have a significant lack-of-fit ($p<0.05$). This meant that there was no planar component to the gain field, but the activity did vary with eye position. Neurons that showed no response to eye position and thus had no gain field (NG), had no significant planar component ($p > 0.05$) and no significant lack-of-fit ($p > 0.05$).

3.3 RESULTS

The neurons were first tested in the characterization tasks for preferred spiral space pattern, preferred laminar motion, and preferred pursuit direction. Then the neurons were tested in the coordinate frame task. We analyzed data from 80 neurons in two monkeys, 51 from monkey DON and 29 from monkey ROY. Neurons were selected for having significant responses in the three conditions of fixed gaze, real pursuit, and simulated pursuit.

3.3.1 Characterization Tasks

3.3.1.1 Spiral Space Tuning

Across the population of MSTd neurons, 74/80 (93%) neurons recorded were significantly tuned to one direction in spiral space ($p<0.05$, Rayleigh test). Figure 3-2A Most of the neurons showed the greatest response to an optic flow pattern that contained an expansion component 69/80 (86%) neurons. The preferred response across the population of neurons was –2° ± 15° (95% confidence interval) and the distribution was not uniform ($p<0.05$, Rayleigh test). However, it is important to note in our study, we selected neurons that showed the greatest response to an expansion pattern. Therefore our population of neurons may not be an accurate representation of the optic flow preferences of neurons in MSTd.

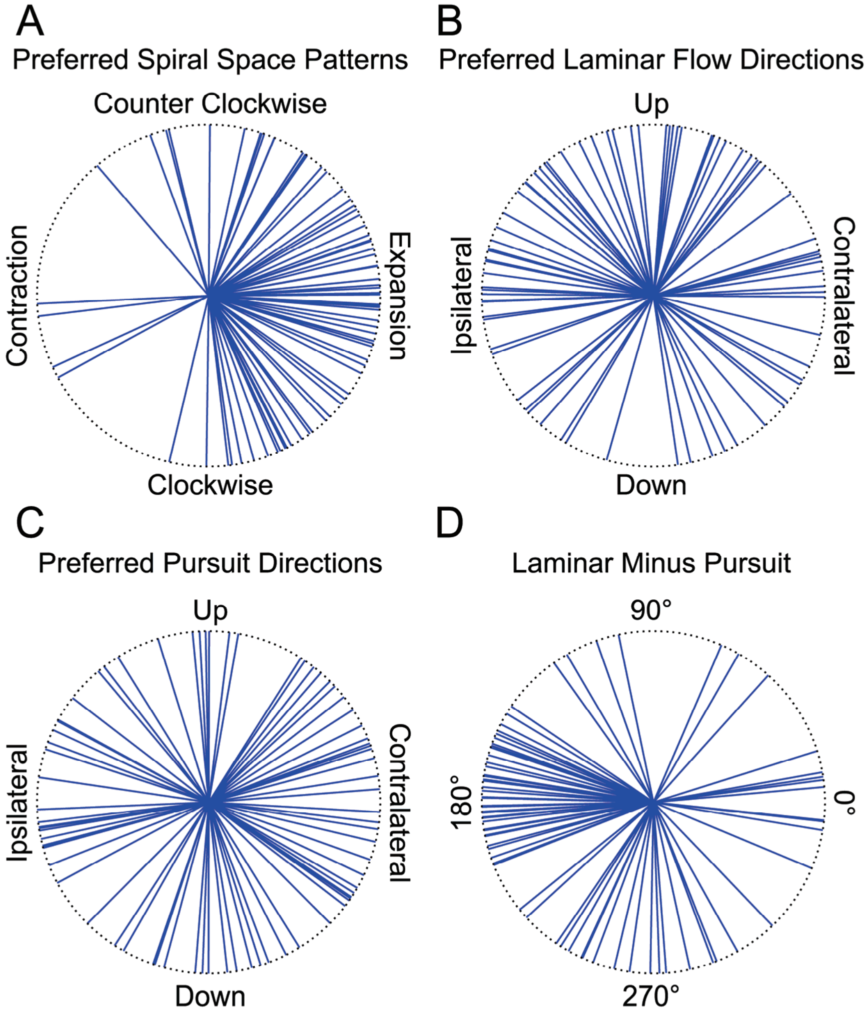

Figure 3-2 Spiral / Laminar / Pursuit / Anti-alignment
A. Spiral space: 74/80 (93%) neurons recorded were significantly tuned to one direction in spiral space ($p<0.05$, Rayleigh test). The preferred response across the population of neurons was –2° ± 15° (95% confidence interval) and the distribution was not uniform ($p<0.05$, Rayleigh test). Most of the neurons showed the greatest response to an optic flow pattern that contained an expansion component 69/80 (86%) neurons.

B. Laminar: 67/80 (84%) MSTd neurons showed significant tuning to laminar motion stimuli ($p<0.05$, Rayleigh test). The distribution of preferred directions was not uniform and was biased towards upward motion ($p<0.05$, Rayleigh test). There was not an ipsilateral / contralateral bias: 40/80 (50%) neurons.

C. Pursuit: 49/80 (61%) MSTd neurons showed significant tuning to pursuit ($p<0.05$, Rayleigh test). The distribution of preferred pursuit directions was not uniform and was biased toward downward motion ($p<0.05$, Rayleigh test). There was also a slight contralateral bias: 42/80 (53%) neurons.

D. Anti-alignment of laminar and pursuit tuning. On a population level, laminar and pursuit tuning showed an anti-alignment of –164° ± 17° (95% confidence interval) and the distribution was not uniform ($p<0.05$, Rayleigh test). Most neurons had an anti-alignment between 90° and 270°: 60/80 (75%) neurons.

3.3.1.2 Laminar Tuning

67/80 (84%) MSTd neurons showed significant tuning to laminar motion stimuli ($p<0.05$, Rayleigh test). Figure 3-2B The distribution of preferred directions was not uniform and was biased towards upward motion ($p<0.05$, Rayleigh test). There was not an ipsilateral / contralateral bias: 40/80 (50%) neurons.

3.3.1.3 Pursuit Tuning

Across the population, 49/80 (61%) MSTd neurons showed significant tuning to pursuit ($p<0.05$, Rayleigh test). Figure 3-2C The distribution of preferred pursuit directions was not uniform and was biased toward downward motion ($p<0.05$, Rayleigh test). There was also a slight contralateral bias: 42/80 (53%) neurons.

3.3.1.4 Anti-alignment of Laminar and Pursuit Tuning

On a population level, laminar and pursuit tuning showed an anti-alignment of $-164° \pm 17°$ (95% confidence interval) and the distribution was not uniform ($p<0.05$, Rayleigh test). Most neurons had an anti-alignment between 90° and 270°: 60/80 (75%) neurons. Figure 3-2D It is possible that the retinal laminar signal and extraretinal pursuit signal are somehow combined to determine heading direction. This anti-alignment is consistent with previous reports (Sakata et al., 1978, 1983; Komatsu and Wurtz, 1988a; Shenoy et al., 2002).

3.3.2 Coordinate Frame Testing

3.3.2.1 Example Neuron: Shift

To determine the coordinate frame of MSTd neurons when the eyes were stationary, we used cross-correlation to measure the shift of the focus tuning curves measured between eye position 1 (–12°) and eye position 5 (12°). These eye positions are the furthest apart so the focus tuning curves are most likely to show the largest shift if the response is not eye-centered. The example neuron in Figure 3-3 has a shift of 0°. This means the focus tuning curve moves with the eye and the neuron is coding in eye coordinates.

The same neuron is plotted in Figure 3-4 with the focus tuning curves overlaid upon each other. The neuron is plotted in both eye coordinates and screen coordinates. The tuning curves will align on top of each other in the coordinate frame in which they are best represented. In the fixed gaze condition, the tuning curves line up exactly in eye coordinates.

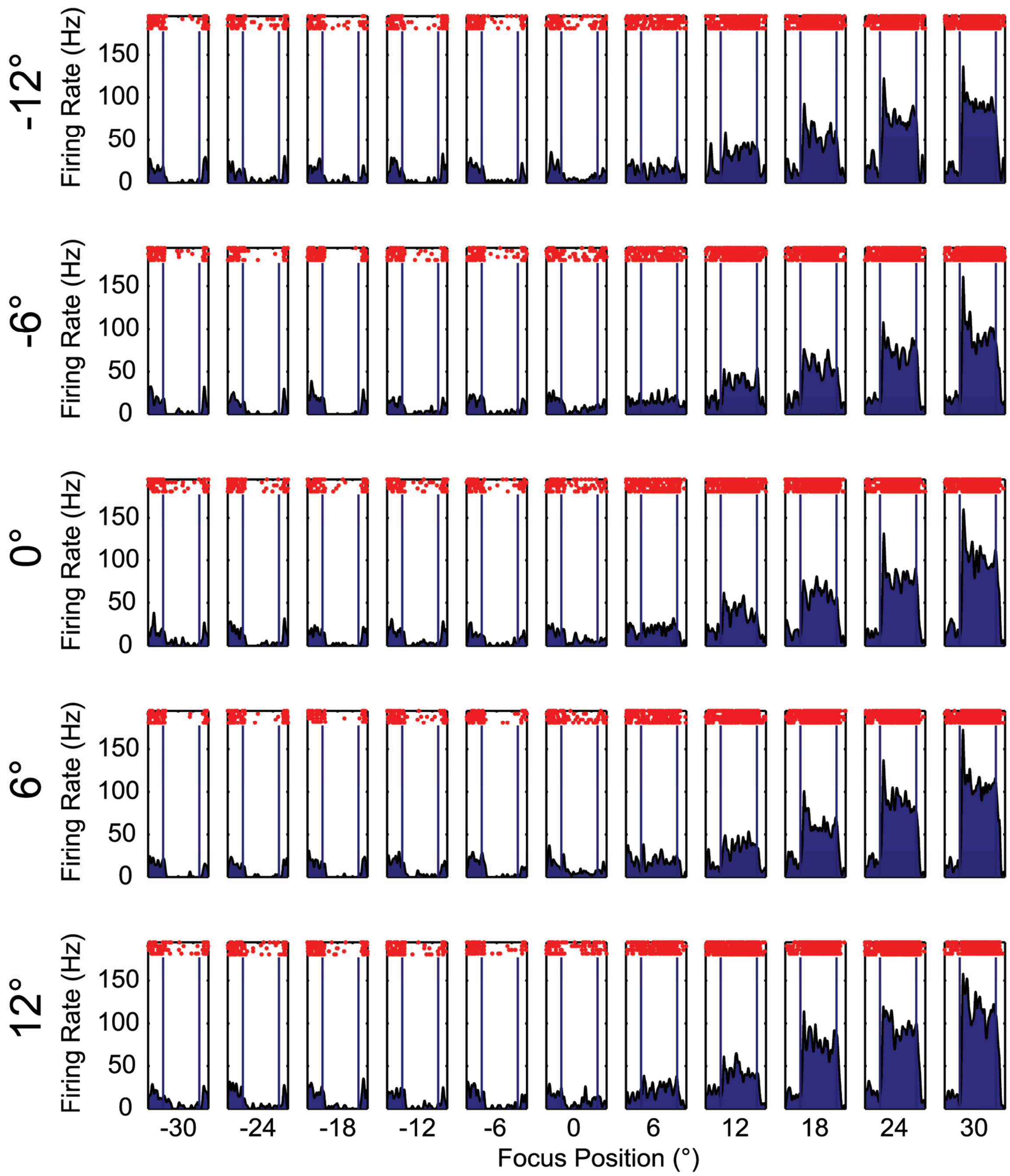

Figure 3-3 PSTH for Five Eye Positions in Fixed Gaze
Raw tuning curves made from several peristimulus time histograms (PSTH) of a single neuron at five eye positions in the fixed gaze condition. Each row is made up of PSTH's which represent the activity of the neuron at each of the 11 focus positions (6° steps, range ± 30°) that make up the heading stimuli. Each row is a different eye position, which range from –12° to 12° in 6° steps. The tuning curves are plotted in eye coordinates and the relative shift from eye position 1 (–12°) to eye position 5 (12°) measured by cross-correlation is 0°. This indicates that this neuron represents focus tuning in eye coordinates.

For the same neuron, when the monkey is pursuing a dot through different eye positions, there is also a 0° shift between eye position 1 and eye position 5. This means that MSTd neurons use the same eye-centered coordinate frame whether the eye is stationary or moving. If the eyes had different coordinate frames depending upon whether the eyes were moving or stationary, this would lead to a rather complicated readout system.

In the simulated pursuit condition where the visual stimulus was dragged across the eyes while they were stationary, there is also zero shift. This condition is behaviorally similar to the fixed gaze condition in that the eyes are not moving, but retinally, it is identical to the real pursuit condition. This result is not unexpected considering that both the fixed gaze and real pursuit conditions demonstrated that MSTd neurons represent heading in eye coordinates.

The cross-correlation analysis indicates that the neurons in MSTd encode the focus of expansion in an eye-centered coordinate frame. However, it is possible the best shift obtained from this analysis was not statistically significant. To test whether the shift at 0° was statistically significant we examined the R-squared value generated from the cross-correlation calculation. If the R-squared value is large, it indicates a 0° shift aligns the focus tuning curves significantly better than chance. We found the vast majority of neurons had a significant 0° shift and so encoded heading in eye coordinates for all three conditions of fixed gaze, real pursuit, and simulated pursuit. (Fixed gaze: 77/80 (96%), real pursuit: 77/80 (96%), simulated pursuit: 74/80 (93%).)

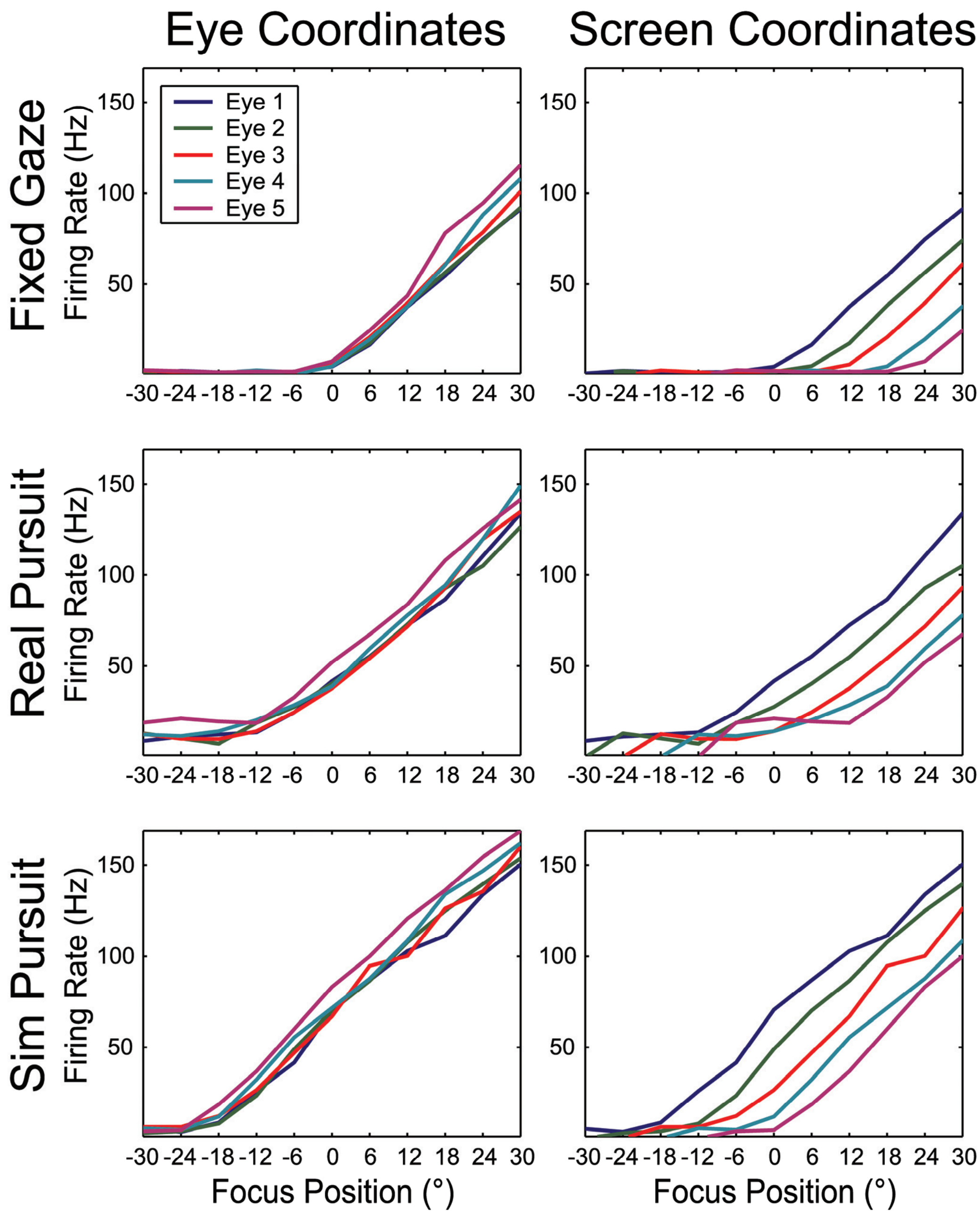

Figure 3-4 Eye / Screen Coordinates Plot
Focus tuning curves from five eye positions overlaid upon each other in eye and screen coordinates for fixed gaze, real pursuit, and simulated pursuit. The Y-axis is the firing rate and the X-axis is the focus position. The tuning curves align with each other in the coordinate frame in which they are represented. This neuron represents focus tuning curves in eye coordinates for all three conditions of fixed gaze, real pursuit, and simulated pursuit. A slight vertical gain effect can be seen, however, the horizontal alignment is 0° in all three task conditions as measured by cross-correlation.

3.3.2.2 Population: Shift Index

To quantify the coordinate frame across the population of neurons, we defined a shift index where 0 = eye coordinates and 1 = screen coordinates. We took the calculated shift between eye position 1 and eye position 5 and divided this by the actual distance between eye position 1 and eye position 5. In the fixed gaze condition, the mean shift index was 0.05 ± 0.04 (95% CI). This shows that the population is coding in eye coordinates. In the real pursuit condition, the mean shift index was –0.02 ± 0.04 (95% CI) and in the simulated pursuit condition, the mean shift index was 0.06 ± 0.04 (95% CI). In all three conditions of fixed gaze, real pursuit, and simulated pursuit, the population of MSTd neurons had a shift index that was not significantly different than 0 and so represented focus tuning in eye coordinates. Figure 3-5

Since we found the majority of neurons in MSTd were encoding in eye coordinates, it was not necessary to test the other coordinates frames (head, body, or world coordinates).

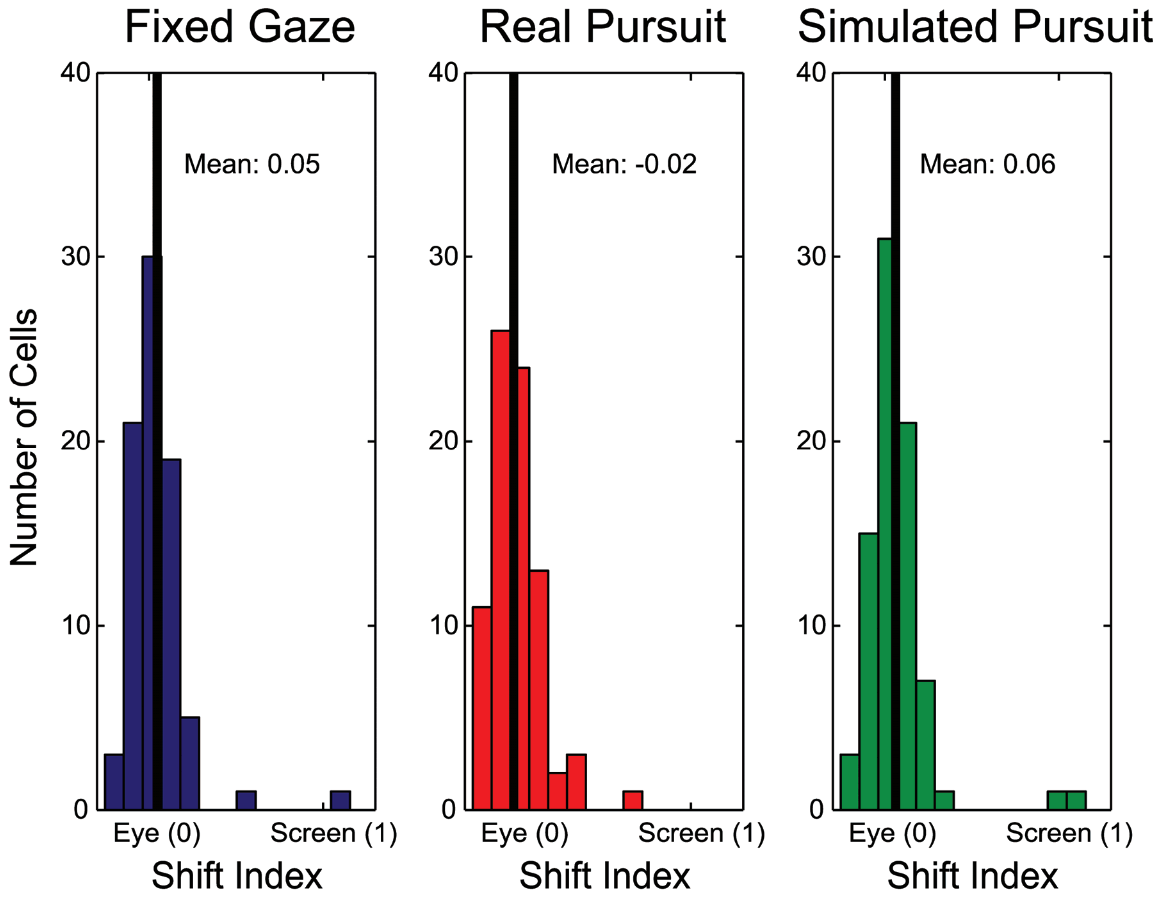

Figure 3-5 Population Shift Index
Shift index for fixed gaze, real pursuit, and simulated pursuit. The shift index is defined as the shift between eye position 1 and eye position 5 divided by the actual distance between eye position 1 and eye position 5 (24°). An index value of 0 indicates the neuron is coding in eye coordinates while a value of 1 indicates screen coordinates. In the fixed gaze condition, the population mean was 0.05 ± 0.04 (95% CI), in real pursuit the mean was –0.02 ± 0.04 (95% CI), and in the simulated pursuit condition the mean was 0.06 ± 0.04 (95% CI). In all three conditions the population of MSTd neurons represent focus tuning curves in eye coordinates.

3.3.3 Gain Analysis

3.3.3.1 Singular Value Decomposition

To test whether there is a multiplicative interaction between eye position and focus of expansion tuning curves, we performed an SVD on the matrix of responses where eye position and focus of expansion were varied. A multiplicative interaction would result if there were an eye position gain field modulation of responses. For responses that showed a multiplicative interaction the SVD estimated the shape of the average tuning curve and gain field. We found that the majority of neurons demonstrated an eye position effect that could be modeled as a gain field in all three conditions. (Fixed gaze: 79/80 (99%) R^2: 0.93 ± 0.07 (mean ± SD), real pursuit: 77/80 (96%) R^2: 0.90 ± 0.08 (mean ± SD), simulated pursuit: 74/80 (93%) R^2: 0.91 ± 0.08 (mean ± SD).)

3.3.3.2 Gain Types

For the neurons that demonstrated a multiplicative interaction, we used linear regression techniques to separate the gain fields into four categories: planar, planar component, no planar component, and no gain (Andersen et al., 1990). This allowed us to identify the shape of the eye position gain fields. Figure 3-6A is an example of a neuron with a planar gain field. Figure 3-6B demonstrates a planar component gain field. Figure 3-6C is a no planar component gain field. The neuron in Figure 3-6D has no gain field.

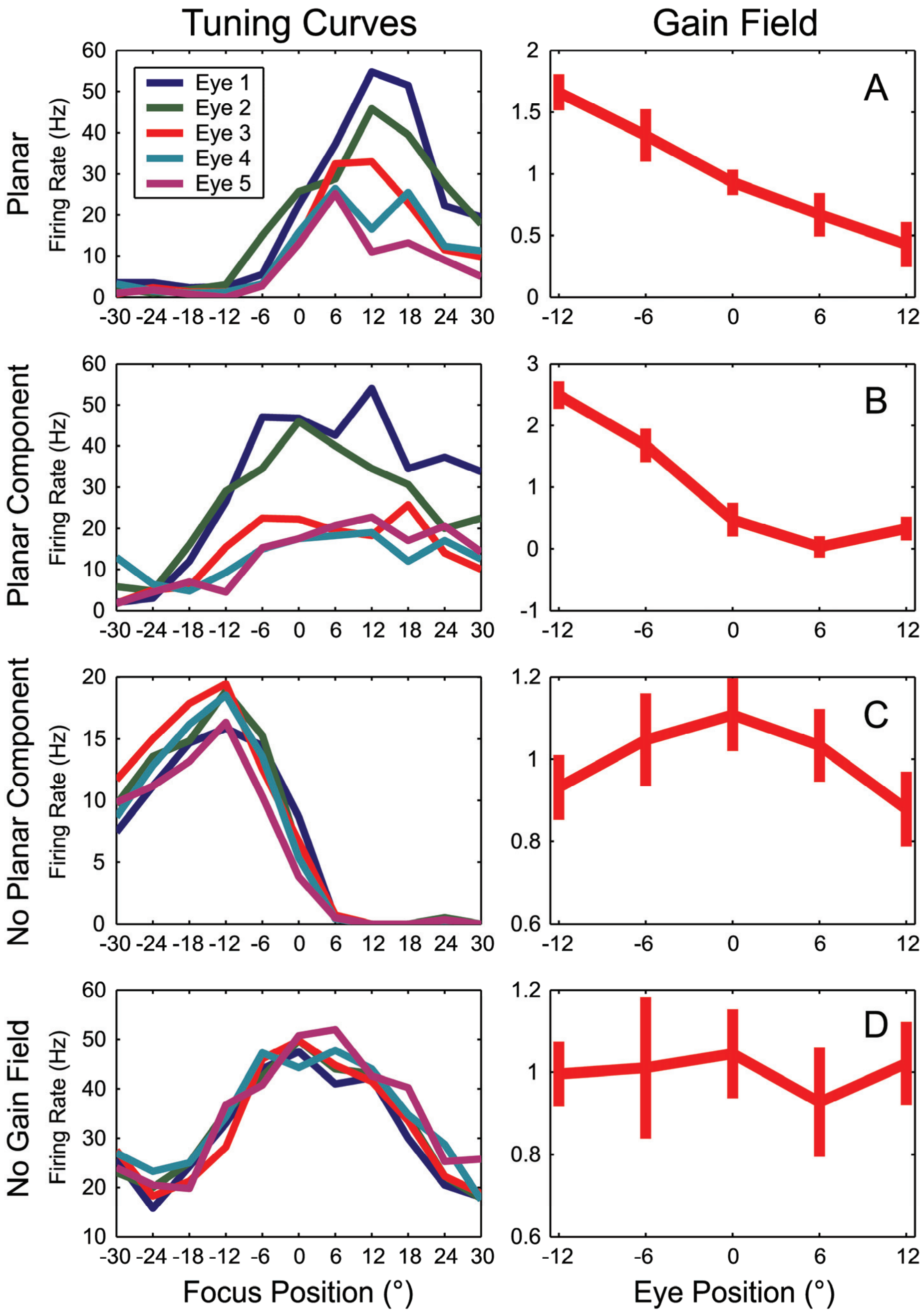

Figure 3-6 Example Gain Fields
Example tuning curves and their respective gain fields. The first column shows the example tuning curves at five eye positions overlaid upon one another while the second column shows the corresponding mean gain field. Error bars are 95% confidence intervals.

The first column in Table 3-1 shows the distribution of gain types for our population of neurons. The second column in Table 3-1 shows the percentages. Neurons that showed no gain effects ranged from 44% to 60% of the neurons depending on the task condition. The third column in Table 3-1 shows the percentages after removing those neurons which have no eye position gain effects. The distribution of planar or planar component neurons versus no planar component neurons is similar in all three task conditions. Approximately two-thirds of the neurons have significant planar or planar component gain fields (~69%). The other one-third (~31%) demonstrate no planar component gain fields. These results are similar to those found in other parietal areas (Andersen et al., 1990).

	Neurons	Percent Includes No Gain	Percent Excludes No Gain
Fixed			
Planar	25/79	32%	57%
Planar Component	5/79	6%	11%
No Planar Component	14/79	18%	32%
No Gain Field	35/79	44%	
Real Pursuit			
Planar	12/77	16%	39%
Planar Component	9/77	12%	29%
No Planar Component	10/77	13%	32%
No Gain Field	46/77	60%	
Simulated Pursuit			
Planar	19/74	26%	44%
Planar Component	12/74	16%	28%
No Planar Component	12/74	16%	28%
No Gain Field	31/74	42%	

Table 3-1 Eye Position Gain Field Types
Linear regression techniques were used to separate the gain fields into four categories: planar, planar component, no planar component, and no gain. Only neurons that were considered separable by SVD were included for gain analysis. Neurons that had significant planar components ($p<0.05$) and no significant lack-of-fit ($p > 0.05$) were classified as planar (P). Neurons that had a significant planar component ($p<0.05$) but also had a significant lack-of-fit ($p<0.05$) were classified as planar component (PC). No planar component (NO) gain fields had no significant planar component ($p > 0.05$) but did have a significant lack-of-fit ($p<0.05$). Neurons that showed no response to eye position and thus had no gain field (NG), had no significant planar component ($p > 0.05$) and no significant lack-of-fit ($p > 0.05$). Percentages were first calculated including neurons that had no gain fields and then again excluding the neurons with no gain fields.

3.3.3.3 Gain Modulation

In order to quantify the amount of change in the gain fields due to eye position, we calculated the percent modulation as 100 * (1 – min/max) which gives us the percent change of the maximum over the eye position range of 24° (Andersen et al., 1990). For example, a result of 50% means that the activity changed 50% of the maximum activity spanning 24°. Table 3-2

The gain modulation varied from 26% to 50%. These results are similar to those found by Andersen et al., (1990). Gain modulation across all three task conditions was approximately similar. Gain modulation by gain type was slightly higher for planar component. Overall gain modulation for the population was 33%.

Gain Modulation	P	PC	NO	Total	
Fixed Gaze	29%	33%	37%	32%	
Real Pursuit	30%	50%	26%	34%	
Simulated Pursuit	28%	39%	35%	33%	
Total	29%	42%	33%	33%	Overall

Table 3-2 Gain Modulation
P = planar, PC = planar component, NO = no planar component. The gain percent modulation was calculated as 100 * (1 – min/max). This gave us the percent change of the maximum over the eye position range of 24°. The gain modulation across all three task conditions was approximately similar. Gain modulation by gain type was slightly higher for planar component. Overall gain modulation for the population was 33%.

3.4 Discussion

The primary goal of the experiments presented here was to determine the coordinate frame in which MSTd neurons represent heading direction. By having the monkeys fixate at five different eye positions with heading stimuli in the same retinal position, we were able to determine that neurons in MSTd represent heading direction in an eye-centered coordinate frame. This finding is consistent with other posterior parietal areas, which also represent their respective modalities in eye coordinates. In addition, we found MSTd neurons demonstrate a multiplicative modulation of neural responses by eye position, which is also a feature found in other posterior parietal areas.

When aligned in eye coordinates, the focus of expansion tuning curves showed zero shift relative to each other both when the eyes are stationary and moving. If MSTd neurons had instead represented heading in different coordinate frames when the eyes were stationary compared to if they were moving, this would have presented a rather complicated readout mechanisms. Since all three conditions of fixed gaze, real pursuit, and simulated pursuit are represented in eye coordinates, this makes the system less complex and a generalized neural processing and modulation system can be used when the eyes are stationary and moving instead of requiring a different mechanism for each condition.

Through lesion studies in monkeys and humans, it is thought that the posterior parietal cortex plays an important role in spatial perception and visually guided self-motion

(Lynch, 1980; Andersen, 1987, 1989; Stein, 1992). Areas in the posterior parietal cortex have specialized functions such as the lateral intraparietal area for saccades, parietal reach region for reaches, and the anterior intraparietal area for grasping. MSTd neurons have been implicated in processing spatial information for the purpose of visually guided movement. Their response properties are in line with an area that is involved with computing heading direction from optic flow (Duffy and Wurtz, 1991b, a; Lappe and Rauschecker, 1994; Duffy and Wurtz, 1995; Bradley et al., 1996; Shenoy et al., 2002), object motion detection (Tanaka et al., 1993), and the control of smooth pursuit eye movements (Komatsu and Wurtz, 1988b).

Each of these posterior parietal areas is located in a position that takes in visual inputs and then transforms and sends the information to a downstream motor command area. Because each planning region has a different action, it has been suggested that the motor plan for each region is represented in the appropriate coordinate frame most relevant to the movement (Colby, 1998). With all the evidence for the involvement of area MSTd in self-motion computation and heading perception, there was a strong possibility that neurons in MSTd already represented focus tuning curves in body or world coordinates. However, we have shown that area MSTd actually codes in an eye-centered coordinate frame, just like the rest of the posterior parietal cortex.

Since vision is a primary source of information to guide locomotion, there must be a transformation from the image on the retina in eye coordinates, to muscle commands, which are in body or world coordinates. As an area that is involved in self-motion perception, the finding that MSTd neurons represent focus tuning curves in eye coordinates, like many other posterior parietal cortical areas, is not surprising. From an efficiency point of view, it makes sense that many cortical areas code in the same coordinate frame. The lateral intraparietal area (LIP) and posterior reach region (PRR) compensate for intervening saccades to maintain target location in eye coordinates for saccades (LIP) (Gnadt and Andersen, 1988; Duhamel et al., 1992) and reaches (PRR) (Batista et al., 1999).

There are several possible reasons why neurons in MSTd are coding in eye coordinates. The first reason might simply be that MSTd represents an early stage where the information is closer to the input than it is the output. While this may partially be true, the fact that neurons in MSTd can compensate for eye movements that perturb the visual scene, adjust for pursuit speed, and adjust for forward translation speed suggests that MSTd is already prominently involved in heading computation. The visual scene is constantly changing as monkeys move throughout the world. Because MSTd neurons are involved in detection of object motion (Tanaka et al., 1993) and control of eye movements (Komatsu and Wurtz, 1988b), it would be most economical to represent the visual scene in eye coordinates and make the necessary corrections at this early stage than later. By coding in eye coordinates like the rest of the posterior parietal cortex, this common coordinate frame allows the areas that control different actions such as saccades, reaches, and grasps to coordinate efficiently.

We also found that firing rates of MSTd neurons are modulated by eye position. Many MSTd neurons have a multiplicative interaction between the focus of expansion tuning curves and eye position gain fields. This result fits in with other posterior parietal areas, which also show eye position gain effects. It appears that eye position modulation of neural responses is a fairly common mechanism in the posterior parietal cortex. The receptive fields are typically represented in eye coordinates and the response magnitude is modulated by eye position.

However, the way gain was calculated in our study was slightly different from other studies. In our experiments, we determined the focus tuning curve made of 11 points for each eye position and then calculated the gain as a function of the shift of the entire tuning curves relative to one another. Many other studies only used a single condition at each eye position, which resulted in comparing firing rates as gain instead of comparing tuning curves as gain (Galletti and Battaglini, 1989; Andersen et al., 1990; Bremmer et al., 1997). The result is that our gain analysis pooled information across multiple eye positions and estimated the shape of the gain field.

Another difference between the current and previous studies is that we used five eye positions along a line in one-dimension while in the aforementioned studies, eye positions were typically arranged in a 3 x 3 grid in two dimensions. Thus the regression analysis would be different in our condition and may yield different gain types due to curvature of the gain fields in two dimensions. We found four types of eye position gain fields: planar, planar component, no planar component, and no gain field. Most of the gain fields we observed were planar in one dimension; however, the effects of eye position have previously been found to be planar along two-dimensional surfaces as well (Andersen et al., 1990; Bremmer et al., 1997).

Including this present study, it is likely that gain modulation is a general mechanism that is present throughout the posterior parietal cortex. Eye position gain modulation has been found in area V3A (Galletti and Battaglini, 1989), V6 (Galletti et al., 1995), area 7a (Andersen and Mountcastle, 1983; Andersen et al., 1985), and LIP (Andersen et al., 1990).

It is postulated that these cortical areas that demonstrate eye position modulation of neural responses might be involved in transforming a retinocentric representation of the world into a non-retinocentric internal map of the external world. Parietal areas including LIP, area 7, area 5, and PRR are gain modulated by eye, head, and limb positions. These gain fields are a possible mechanism that can transform eye-centered coordinates into the coordinate frame of the effector (Andersen, 1997; Cohen and Andersen, 2002). The gain modulation of activity by eye position found in area MSTd and other parietal areas can lead to a distributed code that can transform eye-centered coordinates into head-centered and body-centered coordinates (Zipser and Andersen, 1988; Pouget and Sejnowski, 1995; Xing and Andersen, 2000).

A number of computational studies gave support to the idea that eye position gain modulation is important in coordinate transformations (Andersen and Zipser, 1988;

Zipser and Andersen, 1988; Goodman and Andersen, 1989, 1990). Andersen et al., (1990) found that the hidden units of a neural network trained to represent positions in head-centered coordinates given eye positions and retinal inputs had similar properties to recorded LIP and 7A neurons.

Area MSTd appears to have characteristics similar to its cortical neighbors, namely coding in eye-centered coordinates and eye position gain modulation. These common properties suggest that there is a shared general mechanism for visual-motor transformations in the posterior parietal cortex involving an eye-centered representation.

Chapter 4: Conclusion

Understanding how the brain computes self-motion from optic flow is clearly an enormous undertaking. However, as researchers continue to perform more experiments, our understanding of area MSTd, and its role in computing self-motion from optic flow, will continue to grow.

4.1 Summary

4.1.1 Translation Speed Compensation Experiments

Area MSTd is involved in the computation of heading direction from the focus of expansion (FOE) of the visual image. Our laboratory previously found that MSTd neurons adjust their focus tuning curves to compensate for shifts in the FOE produced by eye rotation (Bradley et al., 1996) as well as for changes in pursuit speed (Shenoy et al., 2002). In this set of experiments, we investigated whether MSTd neurons are able to adjust their focus tuning curves to compensate for varying translation speeds. We found that neurons in MSTd are able to shift their tuning curves towards the actual direction of heading in order to compensate for the shift of the FOE brought about by changes in translation speed. This was true in both the real and simulated pursuit conditions. We found approximately 70% compensation when the eyes were making a real pursuit movement and 36% compensation in the simulated pursuit condition. These results indicate that extraretinal pursuit signals are important in compensation. However, since the simulated pursuit condition also demonstrated significant compensation, it showed that compensation can result from purely retinal cues as well.

To understand the relationship between translation speed, pursuit speed, and the retinal location of the focus of expansion, we performed a regression analysis to investigate whether MSTd neurons were computing the focus of expansion in accordance with Equation 2-2. We found that very few neurons fit the model where translation speed alone or pursuit speed alone were the sole variable. However, when we regressed our data to the full model described by Equation 2-2, which included both translation speed and pursuit speed, we found that many neurons in MSTd fit the model. This showed that both translation speed and pursuit speed are represented in MSTd and are used for heading computation. However since we did not observe 100% compensation for either real or simulated pursuit, it is possible the neurons in MSTd are doing a calculation that is similar but not functionally identical to Equation 2-2, or the calculations are being done at a lower gain.

The results presented here show that many neurons in MSTd shift their focus tuning curves to adjust for changes in translation speed and indicate that retinal as well as extraretinal signals are used in area MSTd for compensation.

4.1.2 Coordinate Frame Experiments

While studies have found that MSTd neurons are able to shift their tuning curves to represent the direction of heading, as opposed to the retinal image, it was not known in which coordinate frame neurons in MSTd represent heading direction. Self-motion generates visual signals that are initially represented in retinal coordinates as the image is captured on the retina. This visual information is later transformed into body or world coordinates to be used for locomotion. Since optic flow is necessary for navigation, many thought that MSTd neurons might be coding in body or world coordinates.

Our experiments were designed to determine the coordinate frame in which MSTd neurons represent heading direction. Focus tuning curves were generated at five eye positions. If neurons in MSTd were coding in eye coordinates, then the tuning curves would move as the eye moved. However, if MSTd neurons were coding in screen (body or world) coordinates, then the tuning curves would remain fixed relative to the screen independently of where the eyes were fixated. We found that when aligned in eye coordinates, the focus of expansion tuning curves showed zero shift relative to each other. This result indicated that area MSTd represents heading in an eye-centered coordinate frame.

Eye-centered coordinates were found for both the fixed gaze condition where the eyes were stationary, and the real pursuit condition, where the eyes were moving. If area MSTd had instead represented heading in different coordinate frames when the eyes were stationary compared to when they were moving, this would have presented a rather complicated readout scenario. By coding in the same coordinate frame regardless of whether the eyes are moving or stationary makes the system less complex and allows the use of more generalized neural processing and modulation mechanisms. In addition, many other areas of the posterior parietal cortex compensate for eye movements in an eye-centered reference frame. The advantage of this common coordinate frame is that the target locations can be transformed into other coordinate frames at later stages of the visual-motor pathway using eye, head, and body position signals (Andersen et al., 1990; Cohen and Andersen, 2002).

We also found that firing rates of MSTd neurons were modulated by eye position. It appears that gain modulation of neural responses is a fairly common mechanism in the posterior parietal cortex. Parietal areas including LIP, area 7, area 5, and PRR are gain modulated by eye, head, and limb positions. It is possible that these gain fields are a mechanism to transform eye-centered coordinates into the reference frame needed by the final motor output areas (Andersen, 1997; Cohen and Andersen, 2002). The gain modulation of activity by eye position found in area MSTd and other parietal areas can lead to a distributed code that can transform eye-centered coordinates into head-centered and body-centered coordinates (Zipser and Andersen, 1988; Pouget and Sejnowski, 1995; Xing and Andersen, 2000).

Area MSTd appears to have characteristics similar to its cortical neighbors, namely coding in eye-centered coordinates and eye position gain modulation. These common properties suggest that there is a shared general mechanism for visual-motor transformations in the posterior parietal cortex.

4.2 Future Experiments

The results of the experiments presented here suggest future work in this cortical area.

4.2.1 Multiple Electrode Recordings in Area MSTd

It would be interesting to use multiple electrode systems (multiple single electrodes, tetrodes, arrays, etc.) to simultaneously record the responses of MSTd neurons to optic flow. Previous research has found that neurons in MSTd represent spiral space in a continuous fashion across the cortex (Graziano et al., 1994). Gessamen et al., (1997) found the interdigitated columns within MSTd were more prominent and widely spaced for expansion/contraction than for expansion/rotation labeling pairs. Britten (1998) found that neurons that were close to each other have more similar optic flow tuning preferences than neurons that were far apart. Using this information as a starting point, by recording multiple neurons simultaneously, any neural interactions can be examined. Do neighboring MSTd neurons have similar laminar motion and pursuit tuning preferences? Do neurons that are shown the same stimulus demonstrate similar pursuit compensations? It is possible that there is a gradient of compensations for adjacent neurons. Any temporal structure in the response could also be explored. By examining the responses of multiple MSTd neurons simultaneously, we can better understand how the neurons are able to encode heading on a population level.

4.2.2 2D versus 3D Stimuli Compensation Task

In our experiments, we used 2D frontoparallel flow fields that simulated approach to a wall. Using these stimuli, we found only partial compensation in both the monkey neurophysiology and human psychophysical experiments. Upadhyay et al., (2000) found that adding 3D cues such as motion parallax to optic flow displays produced larger responses in MSTd neurons when compared to 2D frontoparallel stimuli. With 3D cues, they found that MSTd neurons not only increased their response, but also displayed stronger heading selectivity. This finding is similar to results found in human psychophysical studies. Crowell and Andersen, (2001) found that humans were able to make more accurate heading judgments during pursuit across stimuli that contained 3D cues than those with 2D cues. It would be interesting to examine whether MSTd neurons can demonstrate complete compensation using a similar ground plane with 3D cues. If compensation is improved or complete, this would indicate that 3D motion parallax cues are being used by MSTd neurons.

4.2.3 Simultaneous Recordings from Area MSTd and MT

The neurons in the middle temporal area (MT), which is also known as V5, are tuned for the direction and speed of moving visual stimuli (Albright, 1984; Mikami et al., 1986b, a). The preferred directions are uniformly distributed; however, centrifugal directions are overrepresented (Albright, 1989). While this would suggest that area MT is involved in self-motion processing, area MT is generally considered a relay station for visual processing, not an area that is involved in the processing of visual motion patterns (Bremmer et al., 2000). However, area MT is the major cortical input into area MSTd. It would be interesting to make simultaneous recordings in area MT and MSTd to investigate how the visual information is being processed at each stage. In this manner, it would be possible to examine the temporal structure and coherence of the neural activity between the two areas.

4.2.4 Simultaneous Recordings from Area MSTd and VIP

Neurons in the ventral intraparietal area (VIP) have many characteristics similar to those in MSTd. Like MSTd, VIP neurons also receive input from area MT (Maunsell and van Essen, 1983; Ungerleider and Desimone, 1986b). Both have large receptive fields and respond to spiral space stimuli (Graziano et al., 1994; Schaafsma and Duysens, 1996). Neurons in both areas are selective for the focus of expansion of the visual field (Lappe et al., 1996). However, area VIP differs from area MSTd in that neurons in area VIP respond to tactile stimuli. Bremmer et al., (2000) suggest that VIP might be encoding motion in the near-extrapersonal space. They argue that objects that are located near the animal during self-motion are potential tactile stimuli in the immediate future. In this manner, visual and tactile responses are necessary for self-motion representation close to the body. Due to the similarities between VIP and MSTd, it would be interesting to simultaneously record from active regions in each area that demonstrate responses to self-motion stimuli. Any coherency and temporal structure in the neural activity could shed light on the functional relationship between these two similar areas.

4.2.5 Gain Fields

Gain fields have been demonstrated in MSTd by Bremmer at al. and in this present study (Bremmer et al., 1997). In the coordinate frame experiment presented in Chapter 3, the retinal stimulus was the same between the real pursuit and simulated pursuit conditions. In both conditions, the stimulus moved across the retina. In the real pursuit condition, the eye pursued across a stationary stimulus, while in the simulated pursuit condition, the stimulus was dragged across the motionless eye. In a future experiment, it would be interesting to examine the gain effects by using stimuli that did not move across the retina in the fixed gaze and real pursuit conditions. In the fixed gaze condition, the stimulus would not be moving with respect to the retina. In the real pursuit condition, the stimulus could be fixed in the same retinal location as the eye by moving the stimuli in the same direction and speed as the eye pursuit movement. In this manner, the only difference between the fixed gaze and real pursuit conditions would be the extraretinal eye pursuit signal. It would then be possible to explore the effect of pursuit eye movements on the gain fields.

4.3 Final Thoughts

As we move through our world, our brains are able to guide us efficiently and accurately through the most complex environments with ease. This effortlessness belies the complexity of the neural circuitry that makes vision-based locomotion possible. It is apparent that without the dorsal aspect of the medial superior temporal area, and its specialized ability to process optic flow, we would all be lost.

REFERENCES

Aggleton JP, Mishkin M (1990) Visual impairments in macaques following inferior temporal lesions are exacerbated selectively by additional damage to superior temporal sulcus. Behavioral Brain Research 39:262–274.

Albright TD (1984) Direction and orientation selectivity of neurons in visual area MT of the macaque. J Neurophysiol 52:1106–1130.

Albright TD (1989) Centrifugal Directional Bias in the Middle Temporal Visual Area (Mt) of the Macaque. Visual Neuroscience 2:177–188.

Andersen RA (1987) The role of the inferior parietal lobule in spatial perception and visual-motor integration., Section I: The nervous system. Higher functions of the brain part 2. Bethesda, MD: American Physiological Society.

Andersen RA (1989) Visual and eye movement functions of the posterior parietal cortex. Annual Rev Neurosci 12:377–403.

Andersen RA (1997) Multimodal integration for the representation of space in the posterior parietal cortex. Phil Trans Royal Soc Bio Sci B:1421–1428.

Andersen RA, Mountcastle VB (1983) The influence of the angle of gaze upon the excitability of the light-sensitive neurons of the posterior parietal cortex. J Neurosci 3:532–548.

Andersen RA, Zipser D (1988) The role of the posterior parietal cortex in coordinate transformations for visual-motor integration. Can J Physiol Pharmacol 66:488–501.

Andersen RA, Essick GK, Siegel RM (1985) Encoding of spatial location by posterior parietal neurons. Science 25:456–458.

Andersen RA, Bradley DC, Shenoy KV (1996) Neural mechanisms for heading and structure from motion perception. In: Symposia on Quantitative Biology, pp 15–25. Cold Spring Harbor: Cold Spring Harbor Laboratory Press.

Andersen RA, Snyder LH, Bradley DC, Xing J (1997) Multimodal representation of space in the posterior parietal cortex and its use in planning movements. Annual Rev Neurosci 20:303–330.

Andersen RA, Bracewell RM, Barash S, Gnadt JW, Fogassi L (1990) Eye position effects on visual, memory, and saccade-related activity in areas LIP and 7a of macaque. J Neurosci 10:1176–1196.

Banks MS, Ehrlich SM, Backus BT, Crowell JA (1996) Estimating heading during real and simulated eye movements. Vision Res 36:431–443.

Batista AP, Buneo CA, Snyder LH, Andersen RA (1999) Reach plans in eye-centered coordinates. Science 285:257–260.

Bradley DC, Maxwell M, Andersen RA, Banks MS, Shenoy KV (1996) Mechanisms of heading perception in primate visual cortex. Science 273:1544–1547.

Braun D, Weber H, Mergner T, Schulte-Monting J (1992) Saccadic reaction times in patients with frontal and parietal lesions. Brain 115:1359–1386.

Bremmer F, Duhamel JR, Ben Hamed S, Graf W (2000) Stages of self-motion processing in primate posterior parietal cortex. Int Rev Neurobiol 44:173–198.

Bremmer F, Ilg UJ, Thiele A, Distler C, Hoffmann KP (1997) Eye position effects in monkey cortex. I. Visual and pursuit-related activity in extrastriate areas MT and MST. J Neurophysiol 77:944–961.

Britten KH (1998) Clustering of response selectivity in the medial superior temporal area of extrastriate cortex in the macaque monkey. Vis Neurosci 15:553–558.

Britten KH, van Wezel RJ (1998) Electrical microstimulation of cortical area MST biases heading perception in monkeys. Nat Neurosci 1:59–63.

Cohen YE, Andersen RA (2002) A common reference frame for movement plans in the posterior parietal cortex. Nature Reviews Neuroscience 3:553–562.

Colby CL (1998) Action-oriented spatial reference frames in cortex. Neuron 20:15–24.

Crowell JA, Andersen RA (2001) Pursuit compensation during self-motion. Perception 30:1465–1488.

Crowell JA, Banks MS, Shenoy KV, Andersen RA (1998) Visual self-motion perception during head turns. Nat Neurosci 1:732–737.

Crowell JA, Maxwell MA, Shenoy KV, Andersen RA (1998b) Retinal and extra-retinal motion signals both affect the extent of gaze-shift compensation (abstract). Invest Opthalmol Vis Sci 39:1093.

Desimone R, Ungerleider LG (1986) Multiple visual areas in the caudal superior temporal sulcus of the macaque. J Comp Neurol 248:164–189.

Draper NR, Smith H (1998) Applied regression analysis, 3rd Edition. New York: Wiley.

Duffy CJ, Wurtz RH (1991a) Sensitivity of MST neurons to optic flow stimuli. II. Mechanisms of response selectivity revealed by small-field stimuli. J Neurophysiol 65:1346–1359.

Duffy CJ, Wurtz RH (1991b) Sensitivity of MST neurons to optic flow stimuli. I. A continuum of response selectivity to large-field stimuli. J Neurophysiol 65:1329–1345.

Duffy CJ, Wurtz RH (1995) Response of monkey MSTd neurons to optic flow stimuli with shifted centers of motion. J Neurosci 15:5192–5208.

Duffy CJ, Wurtz RH (1997) Medial superior temporal area neurons respond to speed patterns in optic flow. J Neurosci 17:2839–2851.

Duhamel JR, Colby CL, Goldberg ME (1992) The updating of the representation of visual space in parietal cortex by intended eye movements. Science 255:90–92.

Erickson RG, Thier P (1991) A neuronal correlate of spatial stability during periods of self-induced visual motion. Exp Brain Res 86:608–616.

Galletti C, Battaglini PP (1989) Gaze-dependent visual neurons in area V3A of monkey prestriate cortex. J Neurosci 9:1112–1125.

Galletti C, Battaglini PP, Fattori P (1995) Eye position influence on the parieto-occipital area PO (V6) of the macaque monkey. Eur J Neurosci 7:2486–2501.

Geesaman BJ, Andersen RA (1996) The analysis of complex motion patterns by form/cue invariant MSTd neurons. J Neurosci 16:4716–4732.

Geesaman BJ, Born RT, Andersen RA, Tootell RB (1997) Maps of complex motion selectivity in the superior temporal cortex of the alert macaque monkey: a double-label 2-deoxyglucose study. Cereb Cortex 7:749–757.

Gibson JJ (1950) The Perception of the Visual World. Boston: Houghton Mifflin.

Gnadt JW, Andersen RA (1988) Memory related motor planning activity in posterior parietal cortex of macaque. Experimental Brain Research 70:216–220.

Goodale MA, Milner AD (1992) Separate visual pathways for perception and action. Trends in Neuroscience 15:20–25.

Goodman SJ, Andersen RA (1989) Microstimulation of a neural-network model for visually guided saccades. Journal of Cognitive Neuroscience 1:317–326.

Goodman SJ, Andersen RA (1990) Algorithm programmed by neural network model for coordinate transformations. In: International Joint Conference on Neural Networks, pp 381–386. San Diego, CA: IEEE Neural Network Council, Ann Arbor, MI.

Graziano MS, Andersen RA, Snowden RJ (1994) Tuning of MST neurons to spiral motions. J Neurosci 14:54–67.

Grigo A, Lappe M (1999) Dynamical use of different sources of information in heading judgments from retinal flow. Journal of the Optical Society of America - Optics Image Science and Vision 16:2079–2091.

Harris JM, Rogers BJ (1999) Going against the flow. Trends Cogn Sci 3:449–450.

Hatsopoulos NG, Warren WH (1991) Visual navigation with a neural network. Neural Networks 4:303.

Heeger DJ, Jepson AD (1992) Subspace methods for recovering rigid motion I: Algorithm and implementation. Int J Comput Vis 7:95–177.

Hildreth EC (1992) Recovering heading for visually-guided navigation. Vision Res 32:1177–1192.

Judge SJ, Richmond BJ, Chu FC (1980) Implantation of magnetic search coils for measurement of eye position: an improved method. Vision Res 20:535–538.

Karnath HO, Schenkel P, Fischer B (1991) Trunk orientation as the determining factor of the "contralateral" deficit in the neglect syndrome and as the physical anchor of the internal representation of body orientation in space. Brain 114:1997–2014.

Kawano K, Sasaki M, Yamashita M (1984) Response properties of neurons in posterior parietal cortex of monkey during visual-vestibular stimulation. I. Visual tracking neurons. J Neurophysiol 51:340–351.

Kawano K, Shidara M, Watanabe Y, Yamane S (1994) Neural activity in cortical area MST of alert monkey during ocular following responses. J Neurophysiol 71:2305–2324.

Kleinbaum DG, Kupper LL (1978) Applied regression analysis and other multivariable methods. North Scituate, MA.: Duxbury Press.

Koenderink JJ, van Doorn AJ (1981) Exterospecific component of the motion parallax field. J Opt Soc Am 71:953–957.

Koenderink JJ, van Doorn AJ (1986) Depth and shape from differential perspective in the presence of bending deformations. J Opt Soc Am Ser A 3:242–249.

Koenderink JJ, van Doorn AJ (1987) Facts on optic flow. Biological Cybernetics 56:247–254.

Komatsu H, Wurtz RH (1988a) Relation of cortical areas MT and MST to pursuit eye movements. III. Interaction with full-field visual stimulation. J Neurophysiol 60:621–644.

Komatsu H, Wurtz RH (1988b) Relation of cortical areas MT and MST to pursuit eye movements. I. Localization and visual properties of neurons. J Neurophysiol 60:580–603.

Lagae L, Maes H, Raiguel S, Xiao DK, Orban GA (1994) Responses of macaque STS neurons to optic flow components: a comparison of areas MT and MST. J Neurophysiol 71:1597–1626.

Lappe M, Rauschecker JP (1994) Heading detection from optic flow. Nature 369:712–713.

Lappe M, Bremmer F, Pekel M, Thiele A, Hoffmann KP (1996) Optic flow processing in monkey STS: a theoretical and experimental approach. J Neurosci 16:6265–6285.

Longuet-Higgins HC, Prazdny K (1980) The interpretation of a moving retinal image. In: Proc Roy Soc Lond B Biol Sci, p 151. London.

Lynch JC (1980) The functional organization of posterior parietal association cortex. Behav Brain Sci 3:485–534.

Lynch JC, Mountcastle VB, Talbot WH, Yin TC (1977) Parietal lobe mechanisms for directed visual attention. J Neurophysiol 40:362–389.

Maunsell JH, van Essen DC (1983) The connections of the middle temporal visual area (MT) and their relationship to a cortical hierarchy in the macaque monkey. J Neurosci 3:2563–2586.

Mikami A, Newsome WT, Wurtz RH (1986a) Motion selectivity in macaque visual cortex. II. Spatiotemporal range of directional interactions in MT and V1. J Neurophysiol 55:1328–1339.

Mikami A, Newsome WT, Wurtz RH (1986b) Motion selectivity in macaque visual cortex. I. Mechanisms of direction and speed selectivity in extrastriate area MT. J Neurophysiol 55:1308–1327.

Neter J, Wasserman W, Kutner MH (1983) Applied linear regression models. Homewood, IL.: R.D. Irwin.

Newsome WT, Wurtz RH, Komatsu H (1988) Relation of cortical areas MT and MST to pursuit eye movements. II. Differentiation of retinal from extraretinal inputs. J Neurophysiol 60:604–620.

Orban GA, Lagae L, Verri A, Raiguel S, Xiao D, Maes H, Torre V (1992) First-order analysis of optical flow in monkey brain. Proc Natl Acad Sci U S A 89:2595–2599.

Pena JL, Konishi M (2001) Auditory spatial receptive fields created by multiplication. Science 292:249–252.

Perrone JA, Stone LS (1994) A model of self-motion estimation within primate extrastriate visual cortex. Vision Res 34:2917–2938.

Pouget A, Sejnowski JT (1995) Spatial representations in the parietal cortex of the monkey: Command functions for operations within extra-personal space. Advances in Neural Information Procedure 7:157–164.

Rieger JH, Lawton DT (1985) Processing differential image motion. J Opt Soc Am A 2:354–360.

Royden CS (1994) Analysis of misperceived observer motion during simulated eye rotations. Vision Res 34:3215–3222.

Royden CS, Banks MS, Crowell JA (1992) The perception of heading during eye movements. Nature 360:583–585.

Royden CS, Crowell JA, Banks MS (1994) Estimating heading during eye movements. Vision Res 34:3197–3214.

Rushton SK, Harris JM, Lloyd MR, Wann JP (1998) Guidance of locomotion on foot uses perceived target location rather than optic flow. Curr Biol 8:1191–1194.

Saito H, Yukie M, Tanaka K, Hikosaka K, Fukada Y, Iwai E (1986) Integration of direction signals of image motion in the superior temporal sulcus of the macaque monkey. J Neurosci 6:145–157.

Sakata H, Shibutani H, Kawano K (1978) Parietal neurons with dual sensitivity to real and induced movements of visual target. Neuroscience Letters 9:165–169.

Sakata H, Shibutani H, Kawano K (1983) Functional properties of visual tracking neurons in posterior parietal association cortex of the monkey. J Neurophysiol 49:1364–1380.

Sakata H, Shibutani H, Kawano K, Harrington TL (1985) Neural mechanisms of space vision in the parietal association cortex of the monkey. Vision Res 25:453–463.

Sakata H, Shibutani H, Ito Y, Tsurugai K (1986) Parietal cortical neurons responding to rotary movement of visual stimulus in space. Exp Brain Res 61:658–663.

Sakata H, Shibutani H, Ito Y, Tsurugai K, Mine S, Kusunoki M (1994) Functional properties of rotation-sensitive neurons in the posterior parietal association cortex of the monkey. Exp Brain Res 101:183–202.

Schaafsma SJ, Duysens J (1996) Neurons in the ventral intraparietal area of awake macaque monkey closely resemble neurons in the dorsal part of the medial superior temporal area in their responses to optic flow patterns. Journal of Neurophysiology 76:4056–4068.

Shenoy KV, Bradley DC, Andersen RA (1999) Influence of gaze rotation on the visual response of primate MSTd neurons. J Neurophysiol 81:2764–2786.

Shenoy KV, Crowell JA, Andersen RA (2002) Pursuit speed compensation in cortical area MSTd. Journal of Neurophysiology 88:2630–2647.

Stein JF (1992) The Representation of Egocentric Space in the Posterior Parietal Cortex. Behavioral and Brain Sciences 15:691–700.

Stone LS, Perrone JA (1996) Translation and rotation trade-off in human visual heading estimation (Abstract). Invest Opthalmol 37:2359.

Tanaka K, Saito H (1989) Analysis of motion of the visual field by direction, expansion/contraction, and rotation cells clustered in the dorsal part of the medial superior temporal area of the macaque monkey. J Neurophysiol 62:626–641.

Tanaka K, Fukada Y, Saito HA (1989) Underlying mechanisms of the response specificity of expansion/contraction and rotation cells in the dorsal part of the medial superior temporal area of the macaque monkey. J Neurophysiol 62:642–656.

Tanaka K, Sugita Y, Moriya M, Saito HA (1993) Analysis of object motion in the ventral part of the medial superior temporal area of the macaque visual-cortex. Journal of Neurophysiology 69:128–142.

Tanaka K, Hikosaka K, Saito H, Yukie M, Fukada Y, Iwai E (1986) Analysis of local and wide-field movements in the superior temporal visual areas of the macaque monkey. J Neurosci 6:134–144.

Thier P, Erickson RC (1992b) Responses of visual tracking neurons from cortical area MST-1 to visual, eye, and head motion. Eur J Neurosci 4:539–553.

Ungerleider LG, Mishkin M (1982) Two cortical visual systems. In: Analysis of Visual Behavior (Ingle DJ, Goodale MA, Mansfield RJW, eds), pp 549–585. Cambridge, MA: MIT Press.

Ungerleider LG, Desimone R (1986a) Projections to the superior temporal sulcus from the central and peripheral field representations of V1 and V2. J Comp Neurol 248:147–163.

Ungerleider LG, Desimone R (1986b) Cortical connections of visual area MT in the macaque. J Comp Neurol 248:190–222.

Upadhyay UD, Page WK, Duffy CJ (2000) MST responses to pursuit across optic flow with motion parallax. J Neurophysiol 84:818–826.

Warren WH (1995) Self-Motion: Visual Perception and Visual Control. New York: Academic.

Warren WH, Hannon DJ (1988) Direction of self-motion is perceived from optical flow. Nature 336:162–163.

Warren WH, Jr., Hannon DJ (1990) Eye movements and optical flow. J Opt Soc Am A 7:160–169.

Warren WH, Jr., Kay BA, Zosh WD, Duchon AP, Sahuc S (2001) Optic flow is used to control human walking. Nat Neurosci 4:213–216.

Xing J, Andersen RA (2000) Memory activity of LIP neurons for sequential eye movements simulated with neural networks. Journal of Neurophysiology 84:651–665.

Zar JH (1996) Biostatistical Analysis, 4 Edition. New Jersey: Prentice Hall.

Zipser D, Andersen RA (1988) A back-propagation programmed network that simulates response properties of a subset of posterior parietal neurons. Nature 331:679–684.